JOURNAL OF THE AMERICAN CHEMICAL SOCIETY

Subscriber access provided by American Chemical Society

Article

# Zwitterionic and Cationic Bis(phosphine) Platinum(II) Complexes: Structural, Electronic, and Mechanistic Comparisons Relevant to Ligand Exchange and Benzene C–H Activation Processes

J. Christopher Thomas, and Jonas C. Peters

*J. Am. Chem. Soc.*, **2003**, 125 (29), 8870-8888• DOI: 10.1021/ja0296071 • Publication Date (Web): 17 June 2003

**Downloaded from http://pubs.acs.org on March 29, 2009**

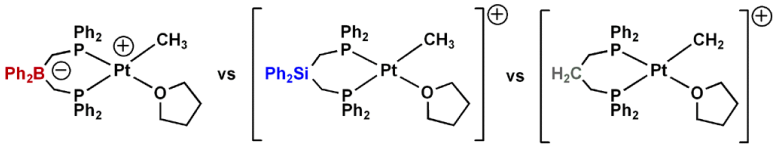


## More About This Article

Additional resources and features associated with this article are available within the HTML version:

- Supporting Information
- Links to the 10 articles that cite this article, as of the time of this article download
- Access to high resolution figures
- Links to articles and content related to this article
- Copyright permission to reproduce figures and/or text from this article

View the Full Text HTML

ACS Publications
High quality. High impact.

Journal of the American Chemical Society is published by the American Chemical Society. 1155 Sixteenth Street N.W., Washington, DC 20036

J|A|C|S
ARTICLES
Published on Web 06/17/2003

# Zwitterionic and Cationic Bis(phosphine) Platinum(II) Complexes: Structural, Electronic, and Mechanistic Comparisons Relevant to Ligand Exchange and Benzene C−H Activation Processes

J. Christopher Thomas and Jonas C. Peters*

*Contribution from the Division of Chemistry and Chemical Engineering, Arnold and Mabel Beckman Laboratories of Chemical Synthesis, California Institute of Technology, Pasadena, California 91125*

Received December 5, 2002; E-mail: jpeters@caltech.edu

***Abstract:*** Structurally similar but charge-differentiated platinum complexes have been prepared using the bidentate phosphine ligands $[Ph_2B(CH_2PPh_2)_2]$, ($[Ph_2BP_2]$, [**1**]), $Ph_2Si(CH_2PPh_2)_2$, ($Ph_2SiP_2$, **2**), and $H_2C(CH_2PPh_2)_2$, (dppp, **3**). The relative electronic impact of each ligand with respect to a coordinated metal center's electron-richness has been examined using comparative molybdenum and platinum model carbonyl and alkyl complexes. Complexes supported by anionic [**1**] are shown to be more electron-rich than those supported by **2** and **3**. A study of the temperature and THF dependence of the rate of THF self-exchange between neutral, formally zwitterionic $[Ph_2BP_2]Pt(Me)(THF)$ (**13**) and its cationic relative $[(Ph_2SiP_2)Pt(Me)(THF)][B(C_6F_5)_4]$ (**14**) demonstrates that different exchange mechanisms are operative for the two systems. Whereas cationic **14** displays THF-dependent, associative THF exchange in benzene, the mechanism of THF exchange for neutral **13** appears to be a THF independent, ligand-assisted process involving an anchimeric, $\eta^3$-binding mode of the $[Ph_2BP_2]$ ligand. The methyl solvento species **13**, **14**, and $[(dppp)Pt(Me)(THF)][B(C_6F_5)_4]$ (**15**), each undergo a C−H bond activation reaction with benzene that generates their corresponding phenyl solvento complexes $[Ph_2BP_2]Pt(Ph)(THF)$ (**16**), $[(Ph_2SiP_2)Pt(Ph)(THF)][B(C_6F_5)_4]$ (**17**), and $[(dppp)Pt(Ph)(THF)][B(C_6F_5)_4]$ (**18**). Examination of the kinetics of each C−H bond activation process shows that neutral **13** reacts faster than both of the cations **14** and **15**. The magnitude of the primary kinetic isotope effect measured for the neutral versus the cationic systems also differs markedly ($k(C_6H_6)/k(C_6D_6)$: **13** = 1.26; **14** = 6.52; **15** ∼ 6). THF inhibits the rate of the thermolysis reaction in all three cases. Extended thermolysis of **17** and **18** results in an aryl coupling process that produces the dicationic, biphenyl-bridged platinum dimers $[\{(Ph_2SiP_2)Pt\}_2(\mu\text{-}\eta^3{:}\eta^3\text{-biphenyl})][B(C_6F_5)_4]_2$ (**19**) and $[\{(dppp)Pt\}_2(\mu\text{-}\eta^3{:}\eta^3\text{-biphenyl})][B(C_6F_5)_4]_2$ (**20**). Extended thermolysis of neutral $[Ph_2BP_2]Pt(Ph)(THF)$ (**16**) results primarily in a disproportionation into the complex molecular salt $\{[Ph_2BP_2]PtPh_2\}^-\{[Ph_2BP_2]Pt(THF)_2\}^+$. The bulky phosphine adducts $[Ph_2BP_2]Pt(Me)\{P(C_6F_5)_3\}$ (**25**) and $[(Ph_2SiP_2)Pt(Me)\{P(C_6F_5)_3\}][B(C_6F_5)_4]$ (**29**) also undergo thermolysis in benzene to produce their respective phenyl complexes, but at a much slower rate than for **13**−**15**. Inspection of the methane byproducts from thermolysis of **13**, **14**, **15**, **25**, and **29** in benzene-$d_6$ shows only $CH_4$ and $CH_3D$. Whereas $CH_3D$ is the dominant byproduct for **14**, **15**, **25**, and **29**, $CH_4$ is the dominant byproduct for **13**. Solution NMR data obtained for **13**, its $^{13}C$-labeled derivative $[Ph_2BP_2]Pt(^{13}CH_3)(THF)$ (**13-$^{13}CH_3$**), and its deuterium-labeled derivative $[Ph_2B(CH_2P(C_6D_5)_2)_2]Pt(Me)(THF)$ (**13-$d_{20}$**), establish that reversible $[Ph_2BP_2]$-metalation processes are operative in benzene solution. Comparison of the rate of first-order decay of **13** versus the decay of $d_{20}$-labeled **13-$d_{20}$** in benzene-$d_6$ affords $k_{13}/k_{13-d20} \sim 3$. The NMR data obtained for **13**, **13-$^{13}CH_3$**, and **13-$d_{20}$** suggest that ligand metalation processes involve both the diphenylborate and the arylphosphine positions of the $[Ph_2BP_2]$ auxiliary. The former type leads to a moderately stable and spectroscopically detectable platinum(IV) intermediate. All of these data provide a mechanistic outline of the benzene solution chemistries for the zwitterionic and the cationic systems that highlights their key similarities and differences.

## I. Introduction

Organometallic cations are ubiquitous in homogeneous catalysis, with applications spanning catalytic C−E bond forming reactions (E = H, C, Si), polymerizations, and alkane activation processes.[1,2] Our group is exploring the chemistry of neutral, formally zwitterionic complexes that are related to reactive organometallic cations supported by conventional phosphine and amine donors.[3] The neutral complexes of interest to us are characterized by (phosphino)- and (amino)borate ligands in which a borate unit is contained within the ligand backbone, partially insulated from the coordinated metal center, so as to preserve reactivity associated with their cationic relatives. Zwitterionic systems of this type may ultimately complement their cationic cousins by virtue of (i) their solubility


10.1021/ja0296071 CCC: $25.00 © 2003 American Chemical Society

and high activity in less polar, noncoordinating solvents, (ii) their potential to show increased tolerance to polar or coordinating functional groups that one might expect to attenuate the reactivity of cationic systems, and (iii) the attenuation of counterion effects which may be present in discrete salt systems.

To begin evaluating this approach to catalysis, it needs to be established whether these neutral systems will give rise to reaction profiles traditionally associated with their cationic analogues. Many factors are likely to impact this issue, but it seems plausible that a borate counteranion rigidly fastened in close proximity to a coordinated metal center will, to some extent, alter the complex's overall reactivity and the operational mechanism by which it mediates a reaction transformation. Therefore, it was of interest to study how the mechanisms of electronically distinct but structurally related neutral and cationic systems compare for a shared organometallic reaction process. Surprisingly little attention has been devoted to such issues previously.[4]

In the present study, we examine the kinetic and mechanistic profiles of structurally related neutral and cationic platinum(II) systems that each mediate an elementary C−H bond activation process in benzene solution. In light of the intense interest in electrophilic C−H activation reactions mediated by late transition metal centers,[5−13] a C−H activation study that compares a neutral with a cationic system is timely. Three platinum(II) systems supported by the structurally related, bidentate phosphine ligands, $[Ph_2BP_2]$ [**1**], $Ph_2SiP_2$ (**2**), and dppp (**3**) (Figure 1) are featured. The major structural difference between complexes supported by [**1**], **2**, and **3** is in the ligand backbone, relatively remote from the phosphine-coordinated metal center. Ligand [**1**] contains an anionic borate unit that, when bound to a $Pt^{II}(X)(L)$ species, affords a neutral and formally zwitterionic $[Ph_2BP_2]Pt(X)(L)$ complex. In this neutral system, the anion is structurally contained within the ligand framework at a distance of ∼4 Å from the coordinated platinum center in the solid-state. Ligand **2** replaces the diphenylborate unit of [**1**] with a structurally similar diphenylsilane unit, and ligand **3** contains the more common methylene backbone. Systems supported by **2** and **3** provide access to more conventional cationic species of the type $[P_2Pt^{II}(X)(L)][X']$, where the primary difference is that, in solution, the counteranion is at an ill-defined distance from the coordinated platinum center with the potential to ion-pair with the metal center. Because a methyl solvento complex of each system proved capable of mediating an elementary benzene C−H bond activation process (Figure 1), the three systems provided an excellent opportunity for a comparative mechanistic study.

Herein, we provide structural, electronic, and kinetic information for the phosphine-supported neutral and cationic platinum(II) systems. We consider these data with respect to the mechanistic profile of each system in benzene solution, and we highlight several important and unexpected mechanistic distinctions between the systems.

## II. Results

**II.1. Synthesis and Characterization of Precursor Complexes.** The syntheses for the anionic borate $[Ph_2BP_2]$ (**1**) and the key neutral complex $[Ph_2BP_2]Pt(Me)(THF)$ (**13**) have been reported previously.[3a] Structurally related complexes were prepared using the neutral ligands $Ph_2Si(CH_2PPh_2)_2$ ($Ph_2SiP_2$, **2**) and 1,3-bis(diphenylphosphino)propane (dppp, **3**). The synthesis of ligand **2** has not been reported but was synthesized readily by addition of two equivalents of $Ph_2PCH_2Li(TMEDA)$ to $Ph_2SiCl_2$ (5.28 g, 82.3% yield). The chemical shifts ($^{31}P$ NMR) for ligands [**1**], **2**, and **3** are shown in Table 1.

Dimethyl platinum(II) complexes of ligands **1**−**3** were obtained by reaction with $(COD)PtMe_2$ in THF. The substitution reactions proceeded cleanly to displace cyclooctadiene and generate $[[Ph_2BP_2]PtMe_2][ASN]$ (**7**),[3a] $(Ph_2SiP_2)PtMe_2$ (**8**), and $(dppp)PtMe_2$ (**9**)[14] in high isolated yield (>90%). Selected NMR data for these three complexes are also presented in Table 1.

(1) For a few examples of cationic metal-mediated bond-forming and polymerization reactions, see: (a) Schrock, R. R.; Osborn, J. A. *J. Am. Chem. Soc.* **1971**, *93*, 3089−3091. (b) Crabtree, R. H. *Acc. Chem. Res.* **1979**, *12*, 331−337. (c) Yasutake, M.; Gridnev, I. D.; Higashi, N.; Imamoto, T. *Org. Lett.* **2001**, *3*, 1701−1704. (d) Oi, S.; Terada, E.; Ohuci, K.; Kato, T.; Tachibana, Y.; Inoue, Y. *J. Org. Chem.* **1999**, *64*, 8660−8667. (e) Ghosh, A. K.; Matsuda, H. *Org. Lett.* **1999**, *1*, 2157−2159. (f) Madine, J. W.; Wang, X.; Widenhoefer, R. A. *Org. Lett.* **2001**, *3*, 385−388. (g) LaPointe, A. M.; Rix, F. C.; Brookhart, M. *J. Am. Chem. Soc.* **1997**, *119*, 906−917. (h) Beletskaya, I. P.; Cheprakov, A. V. *Chem. Rev.* **2000**, *100*, 3009−3066. (i) Ittel, S. D.; Johnson, L. K.; Brookhart, M. *Chem. Rev.* **2000**, *100*, 1169−1203.

(2) Recent summaries and examples of cationic metal-mediated C−H bond activation and functionalization include: (a) Arndtsen, B. A.; Bergman, R. G.; Mobley, T. A.; Peterson, T. H. *Acc. Chem. Res.* **1995**, *28*, 154−162. (b) Lohrenz, J. C. W.; Jacobsen, H. *Angew. Chem., Int. Ed. Engl.* **1996**, *35*, 1305−1307. (c) Sen, A. *Acc. Chem. Res.* **1998**, *31*, 550−557. (d) Stahl, S. S.; Labinger, J. A.; Bercaw, J. E. *Angew. Chem., Int. Ed.* **1998**, *37*, 2181−2192. (e) Balzarek, C.; Weakley, T. J. R.; Tyler, D. R. *J. Am. Chem. Soc.* **2000**, *122*, 9427−9434. (f) Tellers, D. M.; Bergman, R. G. *J. Am. Chem. Soc.* **2000**, *122*, 954−955. (g) Crabtree, R. H. *J. Chem. Soc., Dalton Trans.* **2001**, 2437−2450. (h) Wang, C.; Ziller, J. W.; Flood, T. C. *J. Am. Chem. Soc.* **1995**, *117*, 1647−1648. (i) Shilov, A. E.; Shul'pin, G. B. *Activation and Catalytic Reactions of Saturated Hydrocarbons in the Presence of Metal Complexes*; Kluwer: Boston, 2000.

(3) (a) Thomas, J. C.; Peters, J. C. *J. Am. Chem. Soc.* **2001**, *123*, 5000−5001. (b) Lu, C. C.; Peters, J. C. *J. Am. Chem. Soc.* **2002**, *124*, 5272−5273. (c) Jenkins, D. M.; Betley, T. A.; Peters, J. C. *J. Am. Chem. Soc.* **2002**, *124*, 11 238−11 239. (d) Jenkins, D. M.; Di Bilio, A. J.; Allen, M. J.; Betley, T. A.; Peters, J. C. *J. Am. Chem. Soc.* **2002**, *124*, 15 336−15 350. (e) Brown, S. D.; Betley, T. A.; Peters, J. C. *J. Am. Chem. Soc.* **2003**, *125*, 322−323. (f) Betley, T. A.; Peters, J. C. *Inorg. Chem.* **2002**, *41*, 6541−6543. (g) Betley, T. A.; Peters, J. C. *Angew. Chem., Int. Ed.* **2003**, *42*, 2385−2389.

(4) (a) Hoic, D. A.; Davis, W. M.; Fu, G. C. *J. Am. Chem. Soc.* **1996**, *118*, 8176−8177. (b) Seymore, S. B.; Brown, S. N. *Inorg. Chem.* **2000**, *39*, 325−332. (c) Padilla-Martínez, I. I.; Poveda, M. L.; Carmona, E.; Monge, M. A.; Ruiz-Valero, C. *Organometallics* **2002**, *21*, 93−104.

(5) (a) Stahl, S. S.; Labinger, J. A.; Bercaw, J. E. *J. Am. Chem. Soc.* **1995**, *117*, 9371−9372. (b) Stahl, S. S.; Labinger, J. A.; Bercaw, J. E. *J. Am. Chem. Soc.* **1996**, *118*, 5961−5976.

(6) (a) Holtcamp, M. W.; Labinger, J. A.; Bercaw, J. E. *J. Am. Chem. Soc.* **1997**, *119*, 848−849. (b) Holtcamp, M. W.; Henling, L. M.; Day, M. W.; Labinger, J. A.; Bercaw, J. E. *Inorg. Chim. Acta* **1998**, *270*, 467−478.

(7) Zhong, H. A.; Labinger, J. A.; Bercaw, J. E. *J. Am. Chem. Soc.* **2002**, *124*, 1378−1399.

(8) (a) Wick, D. D.; Goldberg, K. I. *J. Am. Chem. Soc.* **1997**, *119*, 10 235−10 236. (b) Periana, R. A.; Taube, D. J.; Gamble, S.; Taube, H.; Satoh, T.; Fujii, H. *Science* **1998**, *280*, 560−564. (c) Vedernikov, A. N.; Caulton, K. G. *Angew. Chem., Int. Ed.* **2002**, *41*, 4102−4104.

(9) (a) Johansson, L.; Ryan, O. B.; Tilset, M. *J. Am. Chem. Soc.* **1999**, *121*, 1974−1975. (b) Heiberg, H.; Johannson, L.; Gropen, O.; Ryan, O. B.; Swang, O.; Tilset, M. *J. Am. Chem. Soc.* **2000**, *122*, 10 831−10 845. (c) Johansson, L.; Tilset, M.; Labinger, J. A.; Bercaw, J. E. *J. Am. Chem. Soc.* **2000**, *122*, 10 846−10 855. (d) Johannson, L.; Tilset, M. *J. Am. Chem. Soc.* **2001**, *123*, 739−740. (e) Johansson, L.; Ryan, O. B.; Rømming, C.; Tilset, M. *J. Am. Chem. Soc.* **2001**, *123*, 6579−6590.

(10) (a) Reinartz, S.; White, P. S.; Brookhart, M.; Templeton, J. L. *Organometallics* **2001**, *20*, 1709−1712. (b) Reinartz, S.; White, P. S.; Brookhart, M.; Templeton, J. L. *J. Am. Chem. Soc.* **2001**, *123*, 12 724−12 725.

(11) Other phosphine-supported platinum(II) systems which have demonstrated C−H bond activation include: (a) Brainard, R. L.; Nutt, W. R.; Lee, T. R.; Whitesides, G. M. *Organometallics* **1988**, *7*, 2379−2386. (b) Peters, R. G.; White, S.; Roddick, D. M. *Organometallics* **1998**, *17*, 4493−4499. (c) Edelbach, B. L.; Lachichotte, R. J.; Jones, W. D. *J. Am. Chem. Soc.* **1998**, *120*, 2843−2853. See also ref 12.

(12) Konze, W. V.; Scott, B. L.; Kubas, G. J. *J. Am. Chem. Soc.* **2002**, *124*, 12 550−12 556.

(13) Tellers, D. M.; Yung, C. M.; Arndtsen, B. A.; Adamson, D. R.; Bergman, R. G. *J. Am. Chem. Soc.* **2002**, *124*, 1400−1410.

(14) (a) Appleton, T. G.; Bennett, M. A.; Tomkins, I. B. *J. Chem. Soc., Dalton Trans.* **1976**, 439−446. (b) Smith, Jr., D. C.; Haar, C. M.; Stevens, E. D.; Nolan, S. P.; Marshall, W. J.; Moloy, K. G. *Organometallics* **2000**, *19*, 1427−1433.

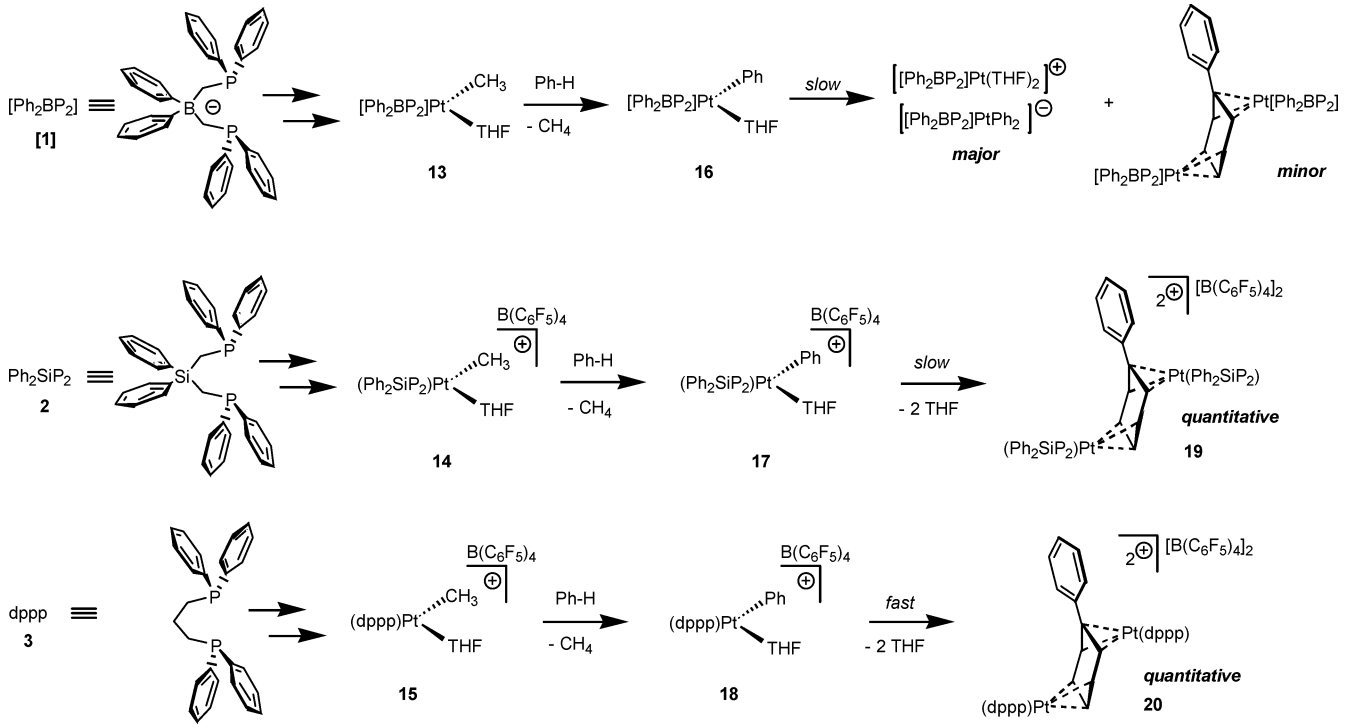


***Figure 1.*** Labeling scheme for the phosphine ligands featured in this paper and the model benzene C−H activation reaction used for the comparative study.

***Table 1.*** Selected NMR Shifts ($\delta$) and Coupling Constants (Hz) for Ligands [**1**], **2**, and **3**, and Platinum Dimethyl Complexes **7**, **8**, and **9** (acetone-$d_6$)

| compound | $^{31}P\{^1H\}$ NMR | $^1J_{Pt-P}$ | $^1H$ NMR Pt-Me | $^3J_{P-H}$ Pt-Me | $^2J_{Pt-H}$ Pt-Me |
|---|---|---|---|---|---|
| $[Ph_2BP_2]$[ASN] [**1**] | −8.78 | | | | |
| $(Ph_2SiP_2)$ (**2**) | −22.65 | | | | |
| dppp (**3**) | −16.29 | | | | |
| $[[Ph_2BP_2]PtMe_2]$[ASN] (**7**) | 20.60 | 1892 | 0.08 (t) | 12 | 68 |
| $(Ph_2SiP_2)PtMe_2$ (**8**) | 12.00 | 1848 | 0.17 (dd) | 6.6, 8.1 | 69 |
| $(dppp)PtMe_2$ (**9**) | 5.47 | 1812 | 0.25 (dd) | 5.4, 6.9 | 69 |

Protonation of the neutral dimethyl species **8** and **9** in dichloromethane in the presence of ca. 40−100 equiv of THF with $[H(Et_2O)_2][B(C_6F_5)_4]$[15] resulted in the clean formation of the salts $[(Ph_2SiP_2)Pt(Me)(THF)][B(C_6F_5)_4]$ (**14**) and $[(dppp)Pt(Me)(THF)][B(C_6F_5)_4]$ (**15**). In comparison to dimethyl complexes **8** and **9**, anionic $[[Ph_2BP_2]PtMe_2]$[ASN] (**7**) was readily protonated by weaker ammonium acids of the type $[HNR_3^+]$, consistent with a more electron-rich, anionic metal center. The cationic methyl solvento complexes **14** and **15** were markedly more stable to both vacuum and halogenated solvents than zwitterionic $[Ph_2BP_2]Pt(Me)(THF)$ (**13**). Complex **13** exhibited decomposition within minutes in dichloromethane at ambient temperature, whereas both **14** and **15** were stable for hours under similar conditions. Also, prolonged exposure of $[Ph_2BP_2]Pt(Me)(THF)$ (**13**) to vacuum resulted in its degradation. Thus, to remove residual THF in the preparation of **13**, it was critical to dry the sample carefully with a gentle stream of argon.

In addition to the precursor methyl solvento complexes **13**−**15**, we also independently prepared and characterized their corresponding phenyl derivatives $[Ph_2BP_2]Pt(Ph)(THF)$[3a] (**16**), $[(Ph_2SiP_2)Pt(Ph)(THF)][B(C_6F_5)_4]$ (**17**), and $[(dppp)Pt(Ph)(THF)][B(C_6F_5)_4]$ (**18**). Compounds **17** and **18** were generated cleanly by protonation of the corresponding diphenyl compounds $(Ph_2SiP_2)PtPh_2$ (**22**) and $(dppp)PtPh_2$[16] (**23**) with $[H(Et_2O)_2][B(C_6F_5)_4]$ in dichloromethane in the presence of ca. 40−100 equiv of THF. The phenyl derivatives **16**, **17**, and **18** proved less thermally stable than their corresponding methyl analogues (vide infra).

**II.2. Structural and NMR Comparisons of 7, 8, 9, and 13.** X-ray diffraction studies were carried out on crystals of the dimethyl complexes **7**−**9** and the neutral methyl solvento complex $[Ph_2BP_2]Pt(Me)(THF)$ (**13**) to confirm their structural analogy. Relevant structural representations are shown in Figure 2, and noteworthy bond lengths and angles are presented in Table 2. As anticipated, the solid-state structures of **7**−**9** are very similar. The Pt−P and Pt−C bond lengths are nearly identical for the three derivatives. The modest deviation observed in the C−Pt−C and P−Pt−P bond angles present in **7**, **8**, and **9** may reflect the presence of a countercation in the unit cell of anionic $[[Ph_2BP_2]PtMe_2]$[ASN] (**7**) that is not present in neutral $(Ph_2SiP_2)PtMe_2$ (**8**) or $(dppp)PtMe_2$ (**9**). The extended lattice structure of **7** (see the Supporting Information) shows that the ammonium cation packs very tightly within the wedge of a diphenylborate unit, and is also in close proximity to the methyl ligands of an adjacent platinum anion. This solid-state arrangement of the cation of **7** may slightly alter the ligand conformation of $[Ph_2BP_2]$ in **7** relative to **8** and **9**. For comparison, the solid-state structure of zwitterionic **13** reveals a P−Pt−P angle (91.96(3)°) that is closer to the bite angles observed for both **8** and **9**.

Another structural parameter of interest concerns the Pt−B distance in (phosphino)borate complexes $[[Ph_2BP_2]PtMe_2]$[ASN] (**7**) and $[Ph_2BP_2]Pt(Me)(THF)$ (**13**). The borate anion in **7** is well-separated from the Pt-center at 4.117(1) Å. This compares

(15) Jutzi, P.; Müller, C.; Stammler, A.; Stammler, H.-G. *Organometallics* **2000**, *19*, 1442−1444.

(16) (a) Romeo, R.; Scolaro, L. M.; Pluntio, M. R.; Del Zotto, A. *Transition Met. Chem.* **1998**, *23*, 789−793. (b) Alibrandi, G.; Bruno, G.; Lanza, S.; Minniti, D.; Romeo, R.; Tobe, M. L. *Inorg. Chem.* **1987**, *26*, 185−190.

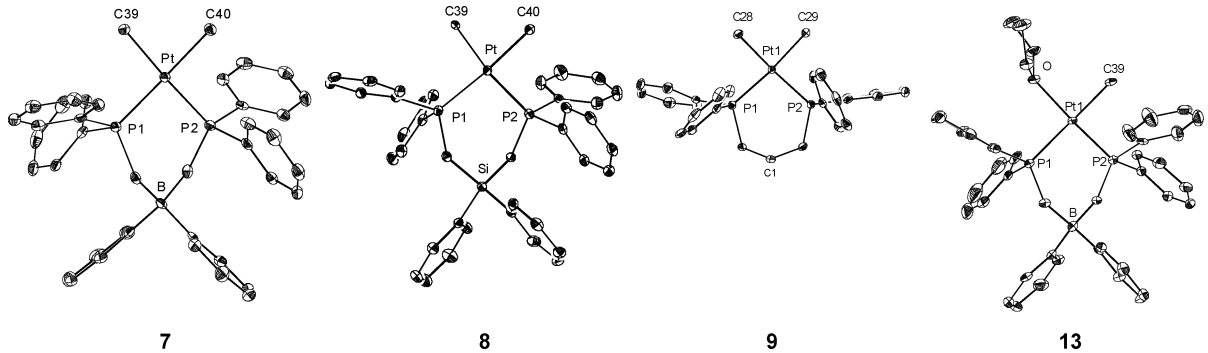


***Figure 2.*** 50% displacement ellipsoid representations of platinum dimethyl complexes [[$Ph_2BP_2$]$PtMe_2$][ASN] (**7**), ($Ph_2SiP_2$)$PtMe_2$·toluene (**8**·toluene), (dppp)$PtMe_2$ (**9**), and platinum methyl solvento complex [$Ph_2BP_2$]Pt(Me)(THF)·2THF (**13**·2THF). Hydrogen atoms, counterions (ASN, **7**), and solvent molecules (toluene, **8**; 2 THF, **13**) are omitted for clarity.

***Table 2.*** Selected Bond Lengths (Å) and Angles (deg) for Complexes **7**, **8**, **9**, and **13**

| complex | Pt–C | Pt–P | C–Pt–C | P–Pt–P |
|---|---|---|---|---|
| [[$Ph_2BP_2$]$PtMe_2$][ASN] (**7**) | 2.134(3), 2.132(3) | 2.2829(7), 2.2776(7) | 86.6(1) | 90.64(2) |
| ($Ph_2SiP_2$)$PtMe_2$ (**8**) | 2.142(3), 2.122(3) | 2.2828(7), 2.2804(7) | 83.8(1) | 94.63(3) |
| (dppp)$PtMe_2$ (**9**) | 2.102(3), 2.113(3) | 2.2724(8), 2.2714(8) | 85.9(1) | 94.30(3) |
| [$Ph_2BP_2$]Pt(Me)(THF) (**13**) | 2.087(6) | 2.313(2)[a] | 91.2(1)[b] | 91.94(6) |

[a] P trans to methyl. [b] C−Pt−O angle.

well with the Pt−Si distance in neutral ($Ph_2SiP_2$)$PtMe_2$ (**8**) (4.192(1) Å) and is slightly longer than the relevant Pt−C1 distance (3.838(1) Å) in (dppp)$PtMe_2$ (**9**) due to a slightly puckered chelate ring in the latter. The Pt−B distance contracts only slightly in moving from anionic **7** to zwitterionic **13** (Pt−B = 4.007(6) Å in **13**).

Structural and NMR parameters potentially sensitive to electronic differences between the neutral and cationic systems include the relative Pt−Me and Pt−P bond lengths obtained from the X-ray structures of **7**−**9**, and chemical shifts and coupling constants observed from their NMR spectra. Data of this type can be used to gauge the relative trans influence of a ligand coordinated to a square planar platinum(II) center. Our data establish that the structural parameters are relatively insensitive to the placement of an anionic diphenylborate unit in [[$Ph_2BP_2$]$PtMe_2$][ASN] (**7**) versus incorporation of a neutral diphenylsilane in ($Ph_2SiP_2$)$PtMe_2$ (**8**) (or a neutral methylene in (dppp)$PtMe_2$ (**9**)). The average Pt−C bond lengths between isostructural **7** and **8** are virtually indistinguishable (ca. 2.13 Å), as are their Pt−P bond distances (ca. 2.28 Å) (Table 2), consistent with structural data obtained for various $(Ar_3P)_2PtMe_2$ complexes that have been reported elsewhere.[17] In considering the comparative NMR data, the magnitudes of the $^2J_{Pt-H}$ coupling constants for **7**−**9** are all very similar (68, 69, and 69 Hz respectively, Table 1), as expected.[18] NMR parameters that do show variation among the three systems are the $^{31}P\{^1H\}$ NMR chemical shift, the $^1J_{Pt-P}$ coupling constant, the Pt−($CH_3$)$_2$ chemical shift in the $^1$H NMR spectrum, and the $^3J_{P-H}$ coupling constant (Table 1). The relationship between the electronic nature of a phosphine-coordinated $PtMe_2$ center and the coupling constant $^1J_{Pt-P}$ and the Pt−($CH_3$)$_2$ chemical shift in the $^1$H NMR spectrum has also been examined previously.[18] The trends observed for para-substituted aryl phosphine adducts of dimethyl platinum(II) suggest that $^1J_{Pt-P}$ decreases and the Pt−($CH_3$)$_2$ chemical shift moves downfield for less donating phosphines. Both of these trends are observed in the data presented here, consistent with suggesting that the bis(phosphino)borate ligand [**1**] provides a platinum center that is to some extent more electron-rich than the isostructural derivatives supported by ligands **2** and **3**.

**II.3. Gauging Electronic Effects using Metal Carbonyl Complexes.** In this paper, we often refer to complexes of the type [$Ph_2BP_2$]Pt(X)(L) (e.g., complex **13**) as formally "zwitterionic". We choose this descriptor to highlight that the diphenylborate unit in these systems is not resonance-delocalized to the phosphine donor atoms, at least not by conventional resonance contributors. Regardless of this distinction, charge in both the neutral and cationic complexes, like all covalent systems, is highly distributed and assigning a formal charge to any atom or unit is invariably misleading. We do think, however, that the zwitterionic description for complexes of the type [$Ph_2BP_2$]Pt(X)(L) is beneficial, especially when considering them in a comparative context with respect to their formally cationic cousins [$P_2$Pt(X)(L)]$^+$.

To address the relative electrophilicity between the platinum centers of [$Ph_2BP_2$]Pt(X)(L) and [$P_2$Pt(X)(L)]$^+$ type systems, the platinum(II) methyl carbonyl complexes were generated. A key assumption we make in this paper is that the relative energy of the CO vibration is a reasonable way to gauge whether the [$Ph_2BP_2$] ligand is more electron-releasing than its neutral relatives $Ph_2SiP_2$ and dppp.[19] In a separate paper, the limitations of this assumption are discussed in greater detail.[20] In brief, we underscore the likelihood that electrostatic factors contribute significantly to the overall magnitude of the difference in a CO stretching frequency between a cationic and a neutral complex. However, we also emphasize the ambiguity that arises if one tries to separate electrophilicity from electrostatic factors.

Reaction of the solvento complexes **13**−**15** with excess carbon monoxide in THF ([$Ph_2BP_2$]Pt(Me)(THF), **13**) or di-

(17) Smith, D. C., Jr.; Haar, C. M.; Stevens, E. D.; Nolan, S. P.; Marshall, W. J.; Moloy, K. G. *Organometallics* **2000**, *19*, 1427−1433.
(18) Haar, C. M.; Nolan, S. P.; Marshall, W. J.; Moloy, K. G.; Prock, A.; Giering, W. G. *Organometallics* **1999**, *18*, 474−479.
(19) Tolman, C. A. *J. Am. Chem. Soc.* **1970**, *92*, 2953−2956 and references therein.
(20) Thomas, J. C.; Peters, J. C. *Inorg. Chem.* **2003**, in press.

***Table 3.*** Comparative Infrared Carbonyl Frequencies ($cm^{-1}$) for Model Platinum (**10**−**12**) and Molybdenum (**4**−**6**) Complexes (KBr cell in $CH_2Cl_2$ solution)

| complex | $\nu$(CO) |
|---|---|
| $[Ph_2BP_2]Pt(Me)(CO)$ (**10**) | 2094 |
| $[(Ph_2SiP_2)Pt(Me)(CO)][B(C_6F_5)_4]$ (**11**) | 2118 |
| $[(dppp)Pt(Me)(CO)][B(C_6F_5)_4]$ (**12**) | 2118 |
| $[[Ph_2BP_2]Mo(CO)_4][ASN]$ (**4**) | 2005 |
| $(Ph_2SiP_2)Mo(CO)_4$ (**5**) | 2018 |
| $(dppp)Mo(CO)_4$ (**6**) | 2018 |

***Scheme 1***

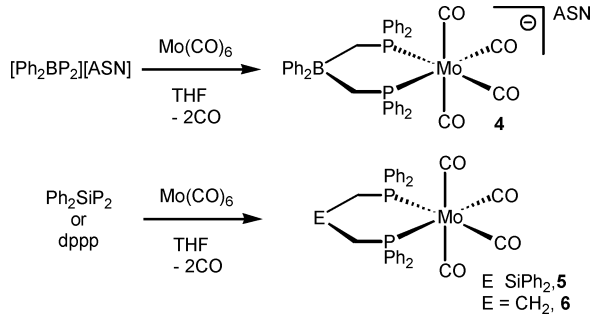


***Scheme 2***

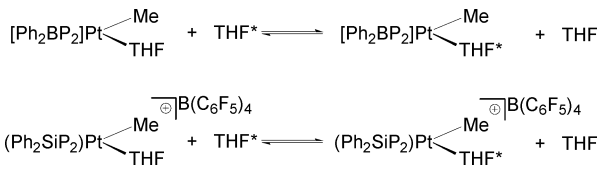


chloromethane ($[(Ph_2SiP_2)Pt(Me)(THF)]^+$, **14**; $[(dppp)Pt(Me)(THF)]^+$, **15**) solution resulted in the rapid formation of the neutral and cationic methyl carbonyl complexes $[Ph_2BP_2]Pt(Me)(CO)$ (**10**), $[(Ph_2SiP_2)Pt(Me)(CO)][B(C_6F_5)_4]$ (**11**), and $[(dppp)Pt(Me)(CO)][B(C_6F_5)_4]$ (**12**), respectively. Solution IR spectra for these derivatives were recorded in dichloromethane in a KBr cell (Table 3). The carbonyl stretching frequencies observed for the two cations are identical (**11**: 2118 $cm^{-1}$, **12**: 2118 $cm^{-1}$). The neutral complex **10**, however, shows a $\nu$(CO) vibration that is 24 $cm^{-1}$ lower in energy (**10**: 2094 $cm^{-1}$). These data suggest that the neutral complex **10** is more electron-rich, and suggest that the $[Ph_2BP_2]$ ligand is likely more electron-releasing than its neutral analogues.

We also examined the phosphine ligands **1**−**3** within the conventional $L_2Mo(CO)_4$ infrared model system. Crabtree has previously suggested that the highest frequency CO vibration, presumed to be an $a_1$ vibration, in tetracarbonyl molybdenum complexes is a reasonable gauge of the relative electron-releasing/accepting character for a bidentate chelate.[21] Reaction of the appropriate bisphosphine ligand **1**−**3** with $Mo(CO)_6$ in refluxing THF for 24−36 h provided the required species $[[Ph_2BP_2]Mo(CO)_4][ASN]$ (**4**), $(Ph_2SiP_2)Mo(CO)_4$ (**5**), and $(dppp)Mo(CO)_4$[22] (**6**), respectively (Scheme 1). Measurement of their respective IR spectra in dichloromethane solution established a trend similar to that of the platinum system: The highest frequency CO vibration for anionic **4** is 2005 $cm^{-1}$ whereas the same vibration for both **5** and **6** is 2018 $cm^{-1}$. These data are in accord with those obtained for the platinum system, supporting the notion that [**1**] is more electron-releasing.

(21) Anton, D. R.; Crabtree, R. H. *Organometallics* **1983**, *2*, 621−627.
(22) Dietsche, W. H. *Tetrahedron Lett.* **1966**, *49*, 6187−6191.

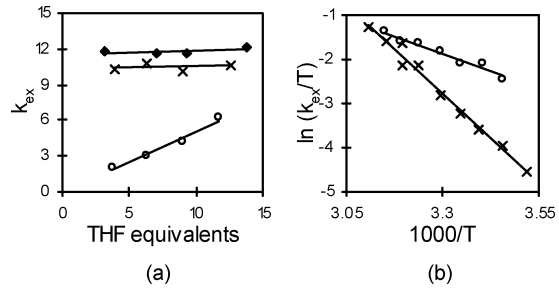


***Figure 3.*** (a) Plot of $k_{ex}$ versus THF equivalents for $[Ph_2BP_2]Pt(Me)(THF)$ (**13**, ×), $[Ph_2B(CH_2P(C_6D_5)_2)_2]Pt(Me)(THF)$ (**13-$d_{20}$**, ◆), and $[(Ph_2SiP_2)Pt(Me)(THF)]^+$ (**14**, ○). (b) Eyring plot of $\ln(k_{ex}/T)$ versus $1000/T$ for neutral methyl solvento complex **13** (×) and cationic methyl solvento complex **14** (○).

**II.4. Determination of Relative THF Ligand Exchange Rates for 13 and 14.** The relative rates and mechanisms of ligand exchange in benzene solution are important to mechanistic considerations discussed in the next section. Measurement of the rate of THF self-exchange for $[Ph_2BP_2]Pt(Me)(THF)$ (**13**) and $[(Ph_2SiP_2)Pt(Me)(THF)]^+$ (**14**) was therefore examined in benzene-$d_6$ in the presence of excess THF through the NMR technique of magnetization transfer using a DANTE pulse sequence[23] (Scheme 2). Saturation of the free downfield THF resonance (ca. 3.6 ppm) transferred intensity to the downfield platinum-bound THF resonance (ca. 2.9 ppm) in each case, and the rate constant for THF exchange ($k_{ex}$) was extracted from the NMR data using the computer program CIFIT.[24]

The dependence of the observed rate constant $k_{ex}$ on the concentration of THF was strikingly different between the neutral and cationic platinum systems. For neutral $[Ph_2BP_2]Pt(Me)(THF)$ (**13**), $k_{ex}$ showed no [THF] dependence over a range of THF concentration (0.146−0.468 M). In sharp contrast, cationic $[(Ph_2SiP_2)Pt(Me)(THF)]^+$ (**14**) showed a first-order dependence on [THF] (0.0766−0.237 M) for the observed rate constant (Figure 3a). The extrapolated intercept for the plot of $k_{ex}$ versus THF equivalents for **14** intersects at the origin and thereby suggests negligible mechanistic dependence on the solvent (benzene) and/or the $[B(C_6F_5)_4]$ anion.[25]

The absolute difference in the rate constant of THF self-exchange ($k_{ex}$) at a given temperature between complex $[Ph_2BP_2]Pt(Me)(THF)$ (**13**) and $[(Ph_2SiP_2)Pt(Me)(THF)]^+$ (**14**) is only modest. For example, at 25 °C, the rate constant for neutral **13** ($k_{ex(298K)}$(**13**) = 12.0 $s^{-1}$) is ∼$^1/_3$ as large as that for cationic **14** ($k_{ex(298K)}$(**14**) = 38.5 $M^{-1}$ $s^{-1}$). More interesting is that the temperature dependence of $k_{ex}$ varies dramatically between **13** and **14**. The rate constant $k_{ex}$ of $[Ph_2BP_2]Pt(Me)(THF)$ (**13**) was examined over the temperature range 11.2−48.9 °C and provided an entropy and enthalpy of activation as follows: $\Delta S^{\ddagger} = 0.1 \pm 5.4$ e.u.; $\Delta H^{\ddagger} = 16.0 \pm 1.6$ kcal/mol (Figure 3b). Analogous data collected for cationic $[(Ph_2SiP_2)Pt(Me)(THF)]^+$ (**14**) over the temperature range 16.0−44.6 °C provided distinctly different values: $\Delta S^{\ddagger} = -30.2 \pm 5.2$ e.u. and $\Delta H^{\ddagger} = 1.9 \pm 0.5$ kcal/mol (Figure 3b).

The activation parameters obtained for $[(Ph_2SiP_2)Pt(Me)(THF)]^+$ (**14**) ($\Delta S^{\ddagger} = -30.2 \pm 5.2$ e.u.; $\Delta H^{\ddagger} = 1.9 \pm 0.5$ kcal/mol) are consistent with a classic associative mechanism

(23) Morris, G. A.; Freeman, R. *J. Magn. Res.* **1978**, *29*, 433−462.
(24) Bain, A. D.; Cramer, J. A. *J. Magn. Res.* **1996**, *118*, 21−27.
(25) Langford, C. H.; Gray, H. B. *Ligand Substitution Processes*; Benjamin: New York, 1966; pp 18−54.

of ligand exchange, in accord with the linear dependence of the exchange rate constant on THF concentration.[25] Associative ligand exchange is commonplace for ligand substitution in square planar platinum(II) systems[25] and is the mechanism we had anticipated for **14**. Particularly noteworthy is that $\Delta H^{\ddagger}$ for **14** suggests that THF exchange is a nearly thermoneutral process—the degree of Pt−O bond making and bond breaking being symmetric in the transition state.

Interpreting the activation parameters and lack of [THF] dependence on $k_{ex}$ of $[Ph_2BP_2]Pt(Me)(THF)$ (**13**) is less straightforward. The remarkable difference in $\Delta H^{\ddagger}$ between **13** and $[(Ph_2SiP_2)Pt(Me)(THF)]^+$ (**14**) reflects a change in mechanism, which could include an energy barrier for significant THF dissociation, or association of a more hindered ligand to displace THF. Perhaps the simplest scenario to put forward for ligand exchange is therefore that of a purely dissociative mechanism that proceeds via a neutral 3-coordinate intermediate, "$[Ph_2BP_2]Pt(Me)$". If the platinum center in $[Ph_2BP_2]Pt(Me)(THF)$ (**13**) is indeed more electron-rich relative to $[(Ph_2SiP_2)Pt(Me)(THF)]^+$ (**14**), then dissociation of a $\sigma$-donor ligand might be expected to be more favorable. However, simple dissociative exchange mechanisms are rarely observed in platinum(II) substitution chemistry.[26a] Even in cases where they have been reported, such as the systems elegantly put forth by Romeo,[26] certain assumptions are required to suggest the presence of a truly 3-coordinate intermediate species. Therefore, two additional mechanisms for THF exchange in $[Ph_2BP_2]Pt(Me)(THF)$ (**13**) need also to be considered: solvolytic displacement of the bound THF from **13** by benzene itself and an anchimeric mechanism whereby a bond pair from the ancillary $[Ph_2BP_2]$ ligand coordinates the platinum center prior to appreciable Pt−O bond breaking. These latter two possibilities constitute associative interchange mechanisms involving discrete 5-coordinate, rather than 3-coordinate, intermediates. Although we cannot distinguish between dissociative, solvent-assisted, or ligand-assisted exchange pathways from the data exchange data alone, the solution NMR data that are discussed below suggest that an anchimeric pathway for ligand exchange is most likely operative for neutral $[Ph_2BP_2]Pt(Me)(THF)$ (**13**).

To probe for the possibility of an isotope-dependent change in the rate of THF self-exchange for neutral $[Ph_2BP_2]Pt(Me)(THF)$ (**13**), we also investigated the $d_{20}$-labeled complex $[Ph_2B(CH_2P(C_6D_5)_2)_2]Pt(Me)(THF)$ (**13-*d*$_{20}$**) (see section II.9c). The [THF] dependence of $k_{ex}$ for THF self-exchange for **13-*d*$_{20}$** was determined at several THF concentrations (0.116−0.497 M) and was found to be independent of [THF] (Figure 3a). The observed rate constant, $k_{ex}$(**13-*d*$_{20}$**) $= 11.6 \pm 0.9\ s^{-1}$ was similar in magnitude to that measured for $[Ph_2BP_2]Pt(Me)(THF)$ (**13**) under similar conditions ($k_{ex}$(**13**) $= 10.3 \pm 2.1\ s^{-1}$).

**II.5. Reaction Pathways of 13, 14, and 15 when Thermolyzed in Benzene between 45 and 55 °C.** As previously reported, $[Ph_2BP_2]Pt(Me)(THF)$ (**13**) reacts in benzene solution at 50 °C over a period of several hours to form $[Ph_2BP_2]Pt(Ph)(THF)$ (**16**) as the major product (∼80%) with concomitant liberation of methane.[3a] The cationic derivatives $[(Ph_2SiP_2)Pt(Me)(THF)]^+$ (**14**) and $[(dppp)Pt(Me)(THF)]^+$ (**15**) reacted similarly, liberating methane to produce the corresponding phenyl derivatives $[(Ph_2SiP_2)Pt(Ph)(THF)]^+$ (**17**) and $[(dppp)Pt(Ph)(THF)]^+$ (**18**) (Figure 1). The phenyl complexes **16**−**18** were not stable to extended thermolysis, as evidenced by the growth of new signals in their respective $^{31}P\{^1H\}$ NMR spectra. Cationic phenyl complexes **17** and **18** each gave rise to quantitative formation of a single new product. Spectroscopic and structural evidence[27] established the products formed to be the orange dinuclear species $[\{(Ph_2SiP_2)Pt\}_2(\mu\text{-}\eta^3{:}\eta^3\text{-biphenyl})][B(C_6F_5)_4]_2$ (**19**) and $[\{(dppp)Pt\}_2(\mu\text{-}\eta^3{:}\eta^3\text{-biphenyl})][B(C_6F_5)_4]_2$ (**20**), the apparent products of a bimolecular aryl coupling process. It is noted that the addition of excess THF significantly inhibited the degradation of pure samples of **16**−**18** in benzene solution. Curiously, whereas complex **19** proved relatively stable to hydrolysis, complex **20** is quite moisture sensitive. During the course of this study, Konze, Scott, and Kubas reported a related coupling reaction for similar cationic bisphosphine platinum(II) complexes; however, the aryl intermediates that presumably result from C−H bond activation processes *were not observed*.[12] We presume that a common mechanism for aryl coupling is prevalent in both sets of systems, but that subtle differences in the bisphosphine ligands give rise to different reaction rates for the step converting the mononuclear phenyl species to their bridged biphenyl products.

Prolonged thermolysis of an independently prepared sample of $[Ph_2BP_2]Pt(Ph)(THF)$ (**16**) resulted in two apparent reaction pathways. The dominant pathway was that of disproportionation to generate the colorless molecular salt $\{[Ph_2BP_2]Pt(Ph)_2\}^-\{[Ph_2BP_2]Pt(THF)_2\}^+$. Formation of this cation/anion pair was suggested by the appearance of two singlets ($^{31}P\{^1H\}$ NMR) in a 1:1 ratio, and by a positive identification of each ion by electrospray mass spectroscopy. Additionally, the species $[[Ph_2BP_2]Pt(Ph)_2][ASN]$ was independently prepared and characterized. A small amount of a presumed bridged-biphenyl species was also evident by $^{31}P\{^1H\}$ NMR and by the orange solution color that developed upon prolonged thermolysis. An independent X-ray diffraction study on crystals of this minor species obtained by fractional crystallization provided connectivity consistent with the dinuclear complex $\{[Ph_2BP_2]Pt\}_2(\mu\text{-}\eta^3{:}\eta^3\text{-biphenyl})$.

**II.6. Benzene C−H Bond Activation Kinetics for 13, 14, and 15.** To evaluate the benzene C−H bond reactivity of the methyl solvento systems $[Ph_2BP_2]Pt(Me)(THF)$ (**13**), $[(Ph_2SiP_2)Pt(Me)(THF)]^+$ (**14**), and $[(dppp)Pt(Me)(THF)]^+$ (**15**), reaction rates were measured under comparative conditions by monitoring the decay of the starting precursors **13**−**15** by either $^{31}P\{^1H\}$ NMR or $^1H$ NMR spectroscopy. The observed rate constants and half-lives are summarized in Table 4, and relevant first-order plots are presented in Figures 4 and 5.

Both $[Ph_2BP_2]Pt(Me)(THF)$ (**13**) and $[(Ph_2SiP_2)Pt(Me)(THF)]^+$ (**14**) displayed clean first-order decay at 45 °C and 55 °C, respectively. The decay of $[(dppp)Pt(Me)(THF)]^+$ (**15**) was more complex. In all cases, the addition of five equivalents of THF slowed the thermal degradation of the starting methyl derivatives, though the attenuation in decay rate was more pronounced for the cations (by ca. a factor of 2). The absence of first-order kinetics for cationic **15** can be attributed to the

(26) (a) Romeo, R. *Comments Inorg. Chem.* **1990**, *11*, 21−57. (b) Romeo, R.; Scolaro, L. M.; Nastasi, N.; Arena, G. *Inorg. Chem.* **1996**, *35*, 5087−5096. (c) Romeo, R.; Alibrandi, G. *Inorg. Chem.* **1997**, *36*, 4822−4830. (d) Romeo, R.; Plutino, M. R.; Elding, L. I. *Inorg. Chem.* **1997**, *36*, 5909−5916. (e) Plutino, M. R.; Scolaro, L. M.; Romeo, R.; Grassi, A. *Inorg. Chem.* **2000**, *39*, 2712−2720.

(27) The results of an X-ray diffraction study of **19** are contained in the Supporting Information.

***Table 4.*** Kinetic Rate Data Fit to a First Order Decay of **13**, **14**, and **15** under Various Conditions

| complex | solvent | $T$ (°C) | additive | rate ($s^{-1}$) | $t_{1/2}$ (min) |
|---|---|---|---|---|---|
| $[Ph_2BP_2]Pt(Me)(THF)$ (**13**) | $C_6H_6$ | 45 | | $1.42(5) \times 10^{-4}$ | 81 |
| | $C_6D_6$ | 45 | | $1.13(3) \times 10^{-4}$ | 102 |
| | $C_6H_6$ | 45 | 5 equiv THF | $9.0(3) \times 10^{-6}$ | 1280 |
| | $C_6H_6$ | 45 | 1 equiv $[^nBu_4N][B(C_6F_5)_4]$ | $1.37(3) \times 10^{-4}$ | 84 |
| | $C_6D_6$ | 55 | | $3.7(2) \times 10^{-4}$ | 31 |
| | $C_6H_6$ | 55 | 5 equiv THF | $3.18(11) \times 10^{-4}$ | 360 |
| $[(Ph_2SiP_2)Pt(Me)(THF)]^+$ (**14**) | $C_6H_6$ | 55 | | $1.80(6) \times 10^{-4}$ | 64 |
| | $C_6D_6$ | 55 | | $2.76(7) \times 10^{-5}$ | 430 |
| | $C_6H_6$ | 55 | 5 equiv THF | $6.0(6) \times 10^{-6}$ | 1900 |
| | $C_6H_6$ | 55 | 1 equiv $[^nBu_4N][B(C_6F_5)_4]$ | $1.34(3) \times 10^{-4}$ | 86 |
| $[(dppp)Pt(Me)(THF)]^+$ (**15**) | $C_6H_6$ | 55 | | $\geq 1.8 \times 10^{-4}$ | $\leq 65$ |
| | $C_6D_6$ | 55 | | $\geq 3.0 \times 10^{-5}$ | $\leq 400$ |
| | $C_6H_6$ | 55 | 5 equiv THF | $4.2(4) \times 10^{-6}$ | 2700 |

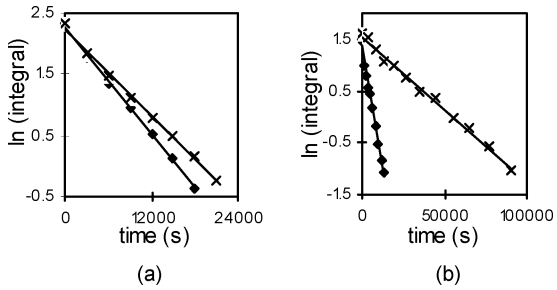


***Figure 4.*** Representative plots of (a) $[Ph_2BP_2]Pt(Me)(THF)$ (**13**) in $C_6H_6$ (◆) and $C_6D_6$ (×) acquired at 45 °C, and (b) $[(Ph_2SiP_2)Pt(Me)(THF)]^+$ (**14**) in $C_6H_6$ (◆) and $C_6D_6$ (×) acquired at 55 °C.

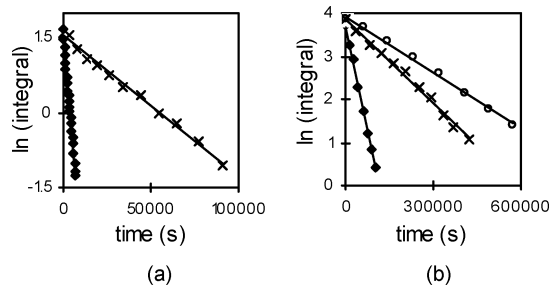


***Figure 5.*** Representative plots of (a) $[Ph_2BP_2]Pt(Me)(THF)$ (**13**) (◆) and $[(Ph_2SiP_2)Pt(Me)(THF)]^+$ (**14**) (×) in $C_6D_6$ acquired at 55 °C, and (b) **13** (◆), **14** (×), and $[(dppp)Pt(Me)(THF)]^+$ (**15**) (○) in $C_6H_6$ with 5 equiv of THF acquired at 55 °C.

kinetically competitive degradation of $[(dppp)Pt(Ph)(THF)]^+$ (**18**) to the biphenyl complex **20**. An inhibitory build-up of THF occurs at such a rate that it complicates the kinetics of **15** by comparison to **13** and **14**.

The effect on the rate of changing the ionic concentration of the solution was examined by the addition of one equivalent of $[^nBu_4N][B(C_6F_5)_4]$. The addition of $[^nBu_4N][B(C_6F_5)_4]$ to $[Ph_2BP_2]Pt(Me)(THF)$ (**13**) had no measurable effect on its rate of decay. However, the rate of decay of $[(Ph_2SiP_2)Pt(Me)(THF)]^+$ (**14**) was slowed somewhat upon inclusion of a stoichiometric equivalent of $[^nBu_4N][B(C_6F_5)_4]$. Worth mentioning is that a second platinum compound was observed by $^{31}P\{^1H\}$ NMR spectroscopy upon addition of 1 equiv of $[^nBu_4N][B(C_6F_5)_4]$ to **14** that represented ~24% of the total integrated phosphorus signal. The spectrum of this secondary species differs only slightly from the starting complex **14**, and it is tempting to assign this secondary species as the anion-coordinated ion-pair $[(Ph_2SiP_2)Pt(Me)]^+[(B(C_6F_5)_4)]^-$; however, we have not been able to rigorously isolate or thoroughly characterize this species.

For each system the benzene thermolysis of **13-15** was carried out in both benzene and benzene-$d_6$. The measured $k(C_6H_6)/k(C_6D_6)$ ratio for $[Ph_2BP_2]Pt(Me)(THF)$ (**13**) at 45 °C was 1.26. We were unable to make a comparable measurement at 55 °C due to the absence of a viable spectroscopic method. This value is strikingly different from that measured for $[(Ph_2SiP_2)Pt(Me)(THF)]^+$ (**14**) and that estimated for $[(dppp)Pt(Me)(THF)]^+$ (**15**) at 55 °C. The measured $k(C_6H_6)/k(C_6D_6)$ ratio for **14** was 6.52 and that for **15** was similar, estimated to be ca. 6 by fitting the decay of **15** to a simple first-order model.

**II.7. Preparation and Benzene Activation Chemistry of Neutral $[Ph_2BP_2]Pt(Me)\{P(C_6F_5)_3\}$ (25) and Cationic $[(Ph_2SiP_2)Pt(Me)\{P(C_6F_5)_3\}][B(C_6F_5)_4]$, (29).** In addition to THF as the coordinatively labile donor L in this study, we also sought a more sterically hindered derivative. We chose the phosphine $P(C_6F_5)_3$ as an appropriate L ligand candidate because of its relatively poor sigma donor ability and its unusually large Tolman cone angle (184°).[28] It also lacks potentially reactive aryl C−H bonds. We found that $P(C_6F_5)_3$ displaced THF from $[Ph_2BP_2]Pt(Me)(THF)$ (**13**) to provide the phosphine adduct complex $[Ph_2BP_2]Pt(Me)\{P(C_6F_5)_3\}$ (**25**) cleanly and in favorable crystalline yield (83%). A structural representation of complex **25**, along with a space filling representation, is shown in Figure 6. It is presumed from the solid-state structure of **25** that the $P(C_6F_5)_3$ coligand, in conjunction with the $[Ph_2BP_2]$ auxiliary, effectively blocks the platinum center with respect to associative approach of a fifth ligand.

Although the platinum center is buried beneath the protective organic aromatic rings, complex $[Ph_2BP_2]Pt(Me)\{P(C_6F_5)_3\}$ (**25**) nonetheless reacts in benzene to quantitatively form the phenyl complex $[Ph_2BP_2]Pt(Ph)\{P(C_6F_5)_3\}$ (**26**) with concomitant liberation of methane (Scheme 3). As might be expected, the benzene C−H activation process is much slower for **25** than for the corresponding THF adduct complex $[Ph_2BP_2]Pt(Me)(THF)$ (**13**). The half-life for **25** was approximately 230 min at 90 °C. The product phenyl complex **26** was also appreciably more stable at this elevated temperature than that of its neutral THF counterpart $[Ph_2BP_2]Pt(Ph)(THF)$ (**16**). The addition of 5 equiv of $P(C_6F_5)_3$ to a benzene solution of **25** significantly attenuated its rate of decay.

The analogous $P(C_6F_5)_3$-ligated cationic complex, $[(Ph_2SiP_2)Pt(Me)\{P(C_6F_5)_3\}][B(C_6F_5)_4]$ (**29**) was prepared by similar means and its thermolysis in benzene-$d_6$ was briefly examined (Scheme 3). Complex **29** underwent conversion to the cationic

(28) Fernandez, A. L.; Wilson, M. R.; Prock, A.; Giering, W. P. *Organometallics* **2001**, *20*, 3429−3435.

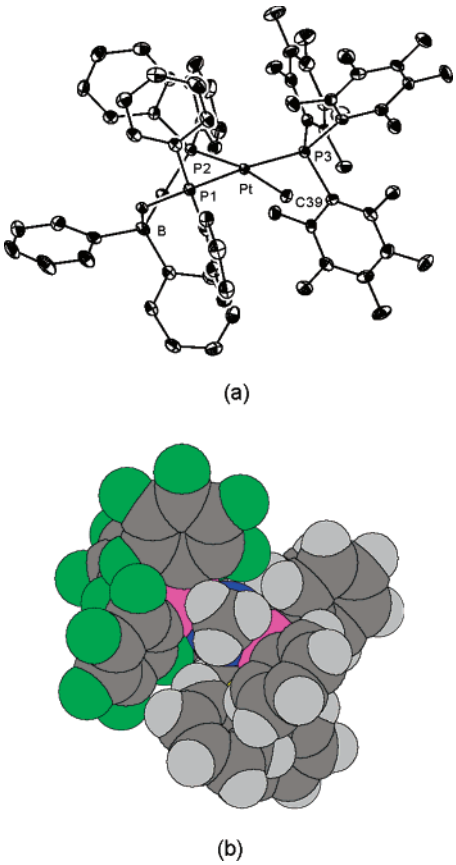


***Figure 6.*** (a) 50% displacement ellipsoid representation of $[Ph_2BP_2]Pt(Me)\{P(C_6F_5)_3\}\cdot C_6H_6$ (**25**·$C_6H_6$). Hydrogen atoms and benzene solvent molecule are omitted for clarity. Selected interatomic distances (Å) and angles (°): Pt−C39, 2.120(3); Pt−P1, 2.3412(12); Pt−P2, 2.3361(10); Pt−P3, 2.2662(12); Pt−B, 3.845(4); C39−Pt−P1, 87.94(9); C39−Pt−P3, 81.40(9); P1−Pt−P2, 86.04(4); P2−Pt−P3, 104.89(4). (b) Space filling representation of **25**, looking down the platinum-methyl bond.

***Scheme 3***

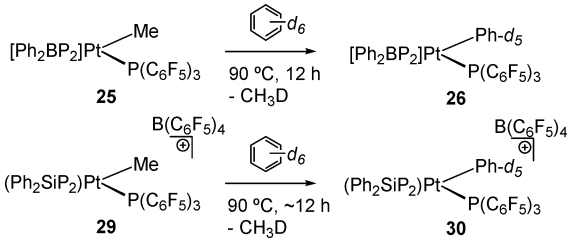


phenyl complex $[(Ph_2SiP_2)Pt(Ph)\{P(C_6F_5)_3\}][B(C_6F_5)_4]$ (**30**) at 90 °C at a rate similar to the conversion of $[Ph_2BP_2]Pt(Me)\{P(C_6F_5)_3\}$ (**25**) to $[Ph_2BP_2]Pt(Ph)\{P(C_6F_5)_3\}$ (**26**). Complex **30** was, however, less stable under the thermolysis conditions and gradually afforded the dinuclear, biphenyl-bridged complex **19**. The collection of accurate rate data was precluded for **29** due to its poor solubility in benzene.

**II.8. Isotopic Incorporation into Methane Byproduct.** The degree of deuterium incorporated into the methane byproduct was determined after thermolysis of complexes **13**−**15**, **25**, and **29** in benzene-$d_6$. The data are presented in Table 5. The nature of the methane byproduct released in the benzene-$d_6$ C−D bond activation reaction was examined by first executing each reaction in a sealed J. Young tube, and then inspecting the methane region of the $^1H$ NMR spectrum after completion of the reaction. The integrated ratio of the methane byproducts reported is taken

***Table 5.*** Methane Isotopomer Ratios Resulting from Thermolysis of Methyl Complexes in Benzene-$d_6$

| compound | *T* (°C) | $CH_4:CH_3D$ |
|---|---|---|
| $[Ph_2BP_2]Pt(Me)(THF)$ (**13**) | 55 | 3.0:1.0 |
| $[Ph_2B(CH_2P(C_6D_5)_2)_2]Pt(Me)(THF)$ (**13-*d*$_{20}$**) | 55 | 1.0:7.3 |
| $[(Ph_2SiP_2)Pt(Me)(THF)]^+$ (**14**) | 55 | 1.0:7.6 |
| $[(dppp)Pt(Me)(THF)]^+$ (**15**) | 55 | 1.0:5.8 |
| $[Ph_2BP_2]Pt(Me)\{P(C_6F_5)_3\}$ (**25**) | 90 | 1.0:5.9 |
| $[(Ph_2SiP_2)Pt(Me)\{P(C_6F_5)_3\}]^+$ (**29**) | 90 | 1.0:5.5 |

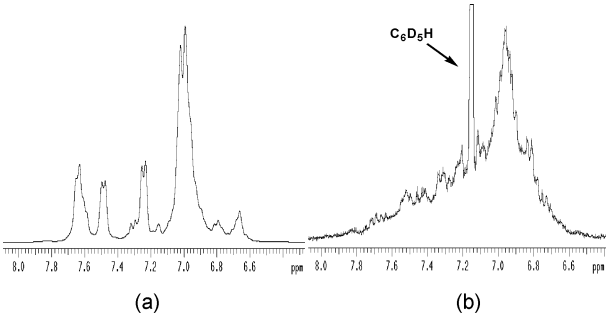


***Figure 7.*** Representative $^1H$ NMR spectra of the aryl region of $[Ph_2BP_2]Pt(Me)(THF)$ (**13**) in benzene-$d_6$ (a) before thermolysis, and (b) after thermolytic conversion to predominantly complex $[Ph_2BP_2]Pt(Ph)(THF)$ (**16**). The complexity of spectrum (b) reflects deuterium incorporation from benzene-$d_6$ into the $[Ph_2BP_2]$ ligand.

as an average of three separate experiments. Only two methane byproducts, $CH_4$ and $CH_3D$, were observed for each of these five systems, and in no case was either isotopomer produced exclusively. The relative ratio of the two byproducts favored $CH_4$ for neutral $[Ph_2BP_2]Pt(Me)(THF)$ (**13**): this result was markedly different from cationic $[(Ph_2SiP_2)Pt(Me)(THF)]^+$ (**14**) and $[(dppp)Pt(Me)(THF)]^+$ (**15**) and the bulky phosphine-ligated complexes $[Ph_2BP_2]Pt(Me)\{P(C_6F_5)_3\}$ (**25**) and $[(Ph_2SiP_2)Pt(Me)\{P(C_6F_5)_3\}]^+$ (**29**), all of which favored $CH_3D$. We also noted that the aryl region of the $^1H$ NMR spectrum of $[Ph_2BP_2]Pt(Me)(THF)$ (**13**) grew increasingly complex during the time course of its thermolysis (Figure 7), suggesting possible deuterium incorporation into the aryl positions of the $[Ph_2BP_2]$ ligand.

**II.9a. Spectral Analysis of Zwitterionic 13 in $C_6D_6$ − Evidence for Intermediate Pt(IV) Species Arising from Reversible Ligand Metalation Processes.** The high degree of $CH_4$ liberated when $[Ph_2BP_2]Pt(Me)(THF)$ (**13**) was incubated in benzene-$d_6$ suggested to us the possibility of reversible $[Ph_2BP_2]$ ligand metalation processes and prompted a closer examination of its $^{31}P\{^1H\}$ and $^1H$ NMR spectra at lower temperature. When a sample of **13** slightly wetted with excess THF was dissolved in benzene-$d_6$, its $^1H$ and $^{31}P\{^1H\}$ NMR spectra revealed complex **13** to be the only detectable solution species. However, when analytically pure **13**, obtained by careful drying under an argon purge to remove residual THF, was dissolved in benzene-$d_6$ and examined at 25 °C by $^{31}P\{^1H\}$ NMR spectroscopy, additional signals were observed that indicated the presence of species distinct from **13**. In contrast to neutral $[Ph_2BP_2]Pt(Me)(THF)$ (**13**), cationic complexes $[(Ph_2SiP_2)Pt(Me)(THF)]^+$ (**14**) and $[(dppp)Pt(Me)(THF)]^+$ (**15**) provided unremarkable NMR spectra at 25 °C in benzene and in benzene-$d_6$, indicative of the presence of a single solution species (see the Supporting Information). Selected regions of the $^{31}P\{^1H\}$ and $^1H\{^{31}P\}$ NMR spectra of **13** in benzene-$d_6$ at 25 °C are shown in Figure 8 to aid their interpretation.

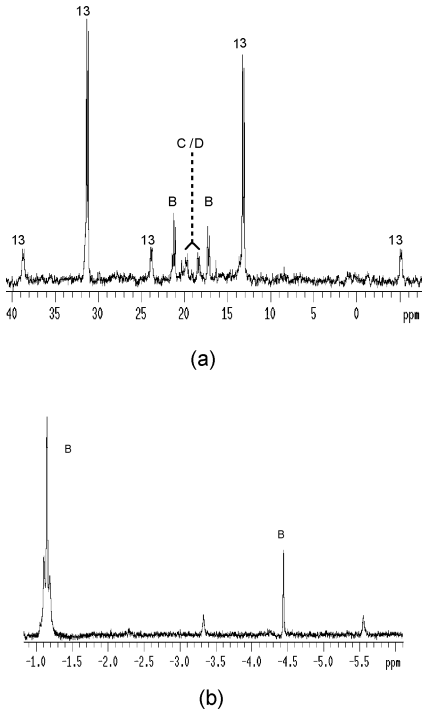


***Figure 8.*** Representative NMR spectra of complex $[Ph_2BP_2]Pt(Me)(THF)$ (**13**) at 25 °C in benzene-$d_6$ showing (a) the $^{31}P\{^1H\}$ NMR containing the expected resonances for **13** and additional resonances corresponding to species **B**, **C** and **D**, and (b) the $^1H\{^{31}P\}$ NMR signals for methyl and hydride resonances assigned to species **B**.

Examination of the $^{31}P\{^1H\}$ NMR spectrum of $[Ph_2BP_2]Pt(Me)(THF)$ (**13**) dissolved in $C_6D_6$ at 25 °C displayed three sets, and possibly a fourth set, of resonances, signifying multiple species in solution. The major set of resonances (labeled **13**; ~80%) appears as two doublets at 34.1 and 16.1 ppm ($^2J_{P-P}$ = 22 Hz), respectively, and corresponds to complex **13**. Another set of signals arising as two doublets centered at 23.0 and 19.3 ppm ($^2J_{P-P}$ = 20 Hz), respectively, labeled **B**, represents ~10% of the total integrated intensity. There is a third, and perhaps fourth, set of resonances in the $^{31}P\{^1H\}$ NMR spectrum (labeled **C** and **D**) centered at 21.7 and 20.4 ppm that can be crudely assigned as doublets with P−P coupling evident ($^2J_{P-P} \approx 20$ Hz). These signals represent only ~5−7% of the total integrated intensity and correspond to possibly two other species.

To further examine the additional species in solution, the $^1H\{^{31}P\}$ NMR spectrum of $[Ph_2BP_2]Pt(Me)(THF)$ (**13**) in $C_6D_6$ was also examined at 25 °C. The $^1H\{^{31}P\}$ NMR spectrum of the same sample reveals a well-defined hydride signal at −4.4 ppm, ($^1J_{Pt-H}$ = 667 Hz), and a distinct methyl resonance at −1.2 ppm with $^{195}Pt$ satellites ($^2J_{Pt-H}$ = 24 Hz) that is well separated from the more intense methyl resonance of **13**. These methyl and hydride resonances appear to correlate to the $^{31}P\{^1H\}$ NMR signals assigned to **B**, in that they all appear to decay at similar rates as $[Ph_2BP_2]Pt(Me)(THF)$ (**13**) is slowly converted to $[Ph_2BP_2]Pt(Ph)(THF)$ (**16**) at 25 °C. Also, the methyl resonance assigned to **B** integrates as three times the intensity of the hydride resonance. Therefore, we assign a hydride, a methyl, and a $[Ph_2BP_2]$ ligand to a single platinum center in **B**, which we think is most consistent with a $[Ph_2BP_2]$-metalated platinum(IV) complex. Because the hydride signal we assign to **B** is present even when the deuterated system $[Ph_2B(CH_2P(C_6D_5)_2)_2]Pt(Me)(THF)$ (**13-*d*$_{20}$**) is examined (vide infra), we suggest that **B** is a

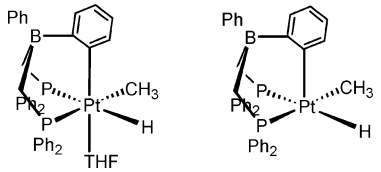


***Figure 9.*** Possible structures for the ortho-metalated platinum(IV) methyl hydride intermediate **B**. 5- and 6-coordinate geometries for **B** can be envisioned.

platinum(IV) product derived from metalation at the diphenylborate unit of the $[Ph_2BP_2]$ ligand, rather than an arylphosphine position. Moreover, the chemical shift and coupling data for the hydride and methyl ligands of **B** are consistent with them being trans to a phosphine donor of the $[Ph_2BP_2]$ ligand.[29] These NMR data are consistent with two possible structures (Figure 9) for the intermediate referred to as **B** that we cannot distinguish. Both 5- and 6-coordinate platinum(IV) species have literature precedent, though 6-coordinate structures are certainly more common.[30]

At least one and possibly two other methyl resonances distinct from those for $[Ph_2BP_2]Pt(Me)(THF)$ (**13**) and **B** could also be distinguished in the $^1H\{^{31}P\}$ NMR spectrum. More data is provided below to verify the presence of four spectroscopically detectable methyl-containing species when pure **13** is dissolved in benzene-$d_6$ at 25 °C. The only well-resolved hydride signal that could be assigned with confidence at 25 °C, however, was that arising from **B**.

**II.9b. Preparation of the $^{13}C$-Labeled Complex $[Ph_2BP_2]Pt(^{13}CH_3)(THF)$ (13-$^{13}CH_3$) and its Characterization by NMR Spectroscopy in Benzene-*d*$_6$ at 25 °C.** As a means to more definitively determine the number of methyl-containing species in solution, we chose to incorporate a $^{13}C$-labeled methyl group into complex $[Ph_2BP_2]Pt(Me)(THF)$ (**13**). Preparation of $[Ph_2BP_2]Pt(^{13}CH_3)(THF)$ (**13-$^{13}CH_3$**) proceeded from the same method as for **13**, using $(COD)Pt(^{13}CH_3)_2$[31] as the starting platinum material.

Dissolving $[Ph_2BP_2]Pt(^{13}CH_3)(THF)$ (**13-$^{13}CH_3$**) in $C_6D_6$ and examining its NMR spectra at 25 °C provided additional information about the species in solution. Definitely three and more likely four distinct sets of platinum-bound methyl resonances could be discerned in the $^1H\{^{31}P\}$ NMR spectrum of **13-$^{13}CH_3$**. The methyl resonances of **13-$^{13}CH_3$** that correlate to those assigned for unlabeled $[Ph_2BP_2]Pt(Me)(THF)$ (**13**) showed the expected $^1J_{C-H}$ coupling arising from the labeled carbon in **13-$^{13}CH_3$**, and the signature $^{195}Pt$ satellites were discernible. The hydride signal at −4.4 ppm remained unchanged by comparison to the unlabeled derivative **13**. We conclude that cis two-bond coupling between the methyl and hydride ligands of species **B** is therefore not resolvable.

The presence of four discrete methyl resonances in the benzene-$d_6$ $^{13}C\{^1H\}$ NMR spectrum of $[Ph_2BP_2]Pt(^{13}CH_3)(THF)$

(29) Puddephatt, R. J. *Coord. Chem. Rev.* **2001**, *219−221*, 157−185.
(30) For examples of 5-coordinate platinum(IV): (a) Ulrich, F.; Kaminsky, W.; Goldberg, K. I. *J. Am. Chem. Soc.* **2001**, *123*, 6423−6424. (b) Ulrich, F.; Goldberg, K. I. *J. Am. Chem. Soc.* **2002**, *124*, 6804−6805. (c) Reinartz, S.; White, P. S.; Brookhart, M.; Templeton, J. L. *J. Am. Chem. Soc.* **2001**, *124*, 6425−6426. For lead references on 6-coordinate platinum(IV): (d) Cotton, F. A.; Wilkinson, G.; Murillo, C. A.; Bochmann, M. *Advanced Inorganic Chemistry*, 6th ed.; John Wiley & Sons: New York, 1999; pp 1080−1082. (e) Roundhill, D. M. In *Comprehensive Coordination Chemistry*, Vol. 5; Wilkinson, G., Gillard, R. D., McCleverty, J. A., Eds.; Pergamon Press: Oxford, 1987; pp 353−531.
(31) Nozaki, K.; Sato, N.; Tonomura, Y.; Yasutomi, M.; Takaya, H.; Hiyama, T.; Matsubara, T.; Koga, N. *J. Am. Chem. Soc.* **1997**, *119*, 12 779−12 795.

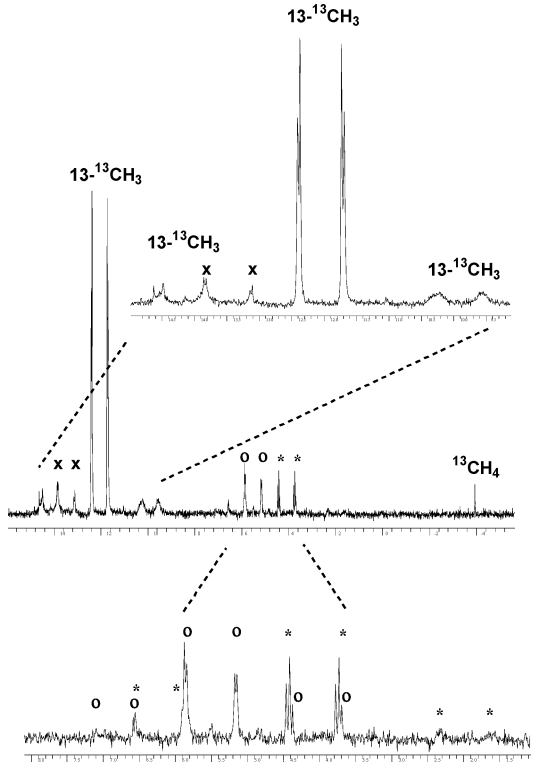


***Figure 10.*** $^{13}C\{^1H\}$ NMR spectrum of $[Ph_2BP_2]Pt(^{13}CH_3)(THF)$ (**13-$^{13}$CH$_3$**) when dissolved in benzene-$d_6$ at 25 °C. The spectrum shows four distinct sets of platinum methyl resonances, the major set corresponding to complex **13-$^{13}$CH$_3$** itself.

(**13-$^{13}$CH$_3$**), presented in Figure 10, corroborates our assignment of four distinct species in the $^{31}P\{^1H\}$ NMR spectrum of $[Ph_2BP_2]Pt(Me)(THF)$ (**13**), although we cannot definitively correlate the observed signals. The $^2J_{C-P}$ coupling can be discerned in each resonance and, in three cases, the $^{195}$Pt satellites are observed. One doublet of doublets at 12.0 ppm (labeled **13-$^{13}$CH$_3$**, $^1J_{Pt-C}$ = 543 Hz, $^2J_{P-C}$ = 4.4, 85 Hz) is consistent with the previously observed methyl for unlabeled $[Ph_2BP_2]Pt(Me)(THF)$ (**13**). Three additional doublets of doublets are also present, and are labeled as x, o, and * in Figure 10. The signal for species x (13.5 ppm, $^2J_{P-C}$ = 5, 90 Hz) is partially obscured by the platinum satellites of the methyl group of **13-$^{13}$CH$_3$**, and its low intensity prevents the detection of platinum coupling. The signals assigned as o and * are separated from **13-$^{13}$CH$_3$** and x, and each displays coupling to one platinum and two phosphorus atoms, arising at 5.5 ppm ($^1J_{Pt-C}$ = 367 Hz, $^2J_{P-C}$ = 5, 88 Hz) and 4.1 ppm ($^1J_{Pt-C}$ = 525 Hz, $^2J_{P-C}$ = 6, 86 Hz), respectively. Each of these signals displays coupling to $^{31}$P that is consistent with one cis and one trans relationship.

The region between 150 and 400 ppm of the $^{13}C\{^1H\}$ NMR spectrum was also carefully inspected for the presence of any "methylene-hydride" type species, such as $[Ph_2BP_2]Pt{=}CH_2(H)$, that might arise from α-hydride migration processes exhibited by $[Ph_2BP_2]Pt(^{13}CH_3)(THF)$ (**13-$^{13}$CH$_3$**). No evidence for any such species was obtained. Formation of a carbene-hydride species from a THF activation process with concomitant expulsion of methane would also have been plausible given that such a process was observed for the cationic system $[(TMEDA)Pt(Me)(L)]^+$ (L = $OEt_2$, THF) reported by Holtcamp, Labinger, and Bercaw.[6] Further confirmation that carbene hydrides are not formed in the case of $[Ph_2BP_2]Pt(Me)(THF)$ (**13**) is that the signal due to $^{13}CH_4$ in Figure 10 is very weak. This signal most likely results from very modest benzene or ligand activation at 25 °C during the time course of the data collection (hours). We conclude that the species **B**, **C**, and **D** that were observed in the $^{31}P\{^1H\}$ NMR of **13** each contain a methyl group and are therefore formed *prior to reductive elimination of methane*.

**II.9c. Preparation, Spectroscopic Characterization, and Benzene Reaction Chemistry of the $d_{20}$-Labeled Complex $[Ph_2B(CH_2P(C_6D_5)_2)_2]Pt(Me)(THF)$ (13-$d_{20}$).** We also prepared the $d_{20}$-$[Ph_2BP_2]$ ligand $[Ph_2B(CH_2P(C_6D_5)_2)_2]$ according to Scheme 4. Although $d_{10}$-methyldiphenylphosphine was obtained in very pure form with virtually no detectable aryl protons ($^1$H NMR), subsequent lithiation followed by addition of diphenylchloroborane to form the required borate ligand gave rise to a small degree (<10%) of proton incorporation in the phenyl rings.

The complex $[Ph_2B(CH_2P(C_6D_5)_2)_2]Pt(Me)(THF)$ (**13-$d_{20}$**) was subsequently prepared and studied by $^1$H and $^2$H NMR spectroscopies. Most important was the use of these spectra to aid the assignment of **B**. The hydride signal at −4.4 ppm that appears when $[Ph_2BP_2]Pt(Me)(THF)$ (**13**) is dissolved in benzene-$d_6$ is still present in the $^1$H NMR spectrum of **13-$d_{20}$**: its intensity is not appreciably diminished, as would be expected if the hydride were derived from the *d*-labeled phenylphosphines. The $^2$H NMR spectrum of **13-$d_{20}$** was also scrutinized thoroughly: no platinum deuteride could be detected. As mentioned above, we interpret these data by formulating **B** as a platinum(IV) methyl hydride metalated at the diphenylborate position.

Two other important results were revealed from examination of the rate of benzene C−H bond activation exhibited by $[Ph_2B(CH_2P(C_6D_5)_2)_2]Pt(Me)(THF)$ (**13-$d_{20}$**). The rate of decay of **13-$d_{20}$** was observed in benzene and benzene-$d_6$ at 55 °C, and the half-lives were approximately 54 and 95 min, respectively. This provided an isotope effect of $k(C_6H_6)/k(C_6D_6)$ ∼1.8. Also, the rate of decay of **13-$d_{20}$** was about three times slower than that of unlabeled $[Ph_2BP_2]Pt(Me)(THF)$ (**13**) in benzene-$d_6$ at 55 °C, providing a $k_{13}/k_{13-d20}$ of ∼3 between the two systems. Additionally, the methane byproduct released during the benzene-$d_6$ thermolysis of **13-$d_{20}$** showed predominantly $CH_3D$ (1.0 *$CH_4$*:7.3 *$CH_3D$*) rather than $CH_4$, as was the case for **13** (Table 5). The implication of these labeling results to the overall solution chemistry of **13** will be more thoroughly discussed in the next section. We simply note for now the likelihood that reversible metalation at a phenylphosphine arm of **13** is likely operative, and a contributing factor to the rate of its intermolecular benzene C−H activation chemistry.

Considering the NMR data for $[Ph_2BP_2]Pt(Me)(THF)$ (**13**), $[Ph_2BP_2]Pt(^{13}CH_3)(THF)$ (**13-$^{13}$CH$_3$**), and $[Ph_2B(CH_2P(C_6D_5)_2)_2]Pt(Me)(THF)$ (**13-$d_{20}$**) as a whole, it is possible to assign with confidence the presence of **13** and also intermediate **B**. Species **C** and **D** may represent isomers of a ligand−metalated species, in which we simply do not detect the hydride signals, but we think that they more likely represent stable Pt(II) species where THF is no longer coordinated in the fourth position. Other alternative ligands that would occupy that site include a benzene adduct, an isomer in which the $[Ph_2BP_2]$ ligand is bound $\eta^3$, or perhaps a three-coordinate platinum center, the latter possibility seeming least likely. Given the recent characterization of an

*Scheme 4*

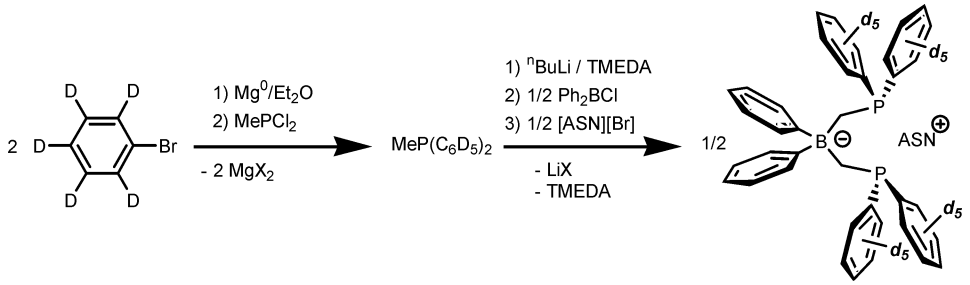


$\eta^2$-benzene adduct of platinum(II)[10b] and that benzene is the solvent, we propose that one of species **C** or **D** is most likely $[Ph_2BP_2]Pt(Me)(\eta^2\text{-benzene})$.

## III. Discussion

**III.1. Comparative Aspects of Benzene C−H Activation Chemistry Exhibited by 13 and 14.** Complexes $[Ph_2BP_2]Pt(Me)(THF)$ (**13**), $[(Ph_2SiP_2)Pt(Me)(THF)]^+$ (**14**), and $[(dppp)Pt(Me)(THF)]^+$ (**15**) each react in benzene to generate the phenyl derivatives $[Ph_2BP_2]Pt(Ph)(THF)$ (**16**), $[(Ph_2SiP_2)Pt(Ph)(THF)]^+$ (**17**), and $[(dppp)Pt(Ph)(THF)]^+$ (**18**), respectively.[11] Our primary aim in this section is to assemble the many pieces of data presented in the results section into a reasonable model that describes the intimate benzene solution chemistry of neutral **13** in comparison to its cationic analogues **14** and **15**. Within this context, we will try to describe the mechanisms by which benzene enters the coordination sphere of the respective platinum centers, the factors that dictate the rate at which it undergoes C−H activation, and the role of the auxiliary phosphine ligand in each case. Because the solution chemistries of cationic **14** and **15** appear to be very similar, we confine our comparative discussion to systems $[Ph_2BP_2]Pt(Me)(THF)$ (**13**) and $[(Ph_2SiP_2)Pt(Me)(THF)]^+$ (**14**) and note by analogy that our conclusions between these two systems map to similar conclusions between **13** and $[(dppp)Pt(Me)(THF)]^+$ (**15**).

The measured rates of first-order decay exhibited by $[Ph_2BP_2]Pt(Me)(THF)$ (**13**) and $[(Ph_2SiP_2)Pt(Me)(THF)]^+$ (**14**) in both benzene and benzene-$d_6$ provided two important pieces of data. First, complex **13** is more reactive toward intermolecular benzene C−H activation than **14**. This was at first surprising. At the outset of our study, much attention was being drawn to increasingly electrophilic platinum systems,[5−12] the rationale being that more electrophilic systems would undergo C−H activation more rapidly. This study, in addition to recent studies by Bercaw[7] and Bergman,[13] establishes that a variety of factors dominate the overall rate of intermolecular C−H activation and that electronic factors can play an indirect, often nonintuitive, role.

Due in part to the pronounced kinetic deuterium isotope effect measured for $[(Ph_2SiP_2)Pt(Me)(THF)]^+$ (**14**), $k(C_6H_6)/k(C_6D_6) = 6.52$ at 55 °C, compared to the modest if not negligible effect measured for $[Ph_2BP_2]Pt(Me)(THF)$ (**13**), $k(C_6H_6)/k(C_6D_6) = 1.26$ at 45 °C, the rate of C−D activation in benzene-$d_6$ is approximately fourteen times faster for **13** than it is for **14** ($t_{1/2}$ at 55 °C = 31 and 430 min, respectively). If we assume that the isotope effect remains relatively constant over temperature, we can extrapolate that the difference in rates in $C_6H_6$ at 55 °C to be small, however, with $[Ph_2BP_2]Pt(Me)(THF)$ (**13**) being about a factor of 2 faster. The measured differences in absolute rate reflect different operative mechanisms and therefore do not clearly provide information concerning how the relative electrophilicities of each system correlate to the rate of the elementary C−H bond-breaking step they each exhibit.

Each case showed a slowing of the rate of C−H activation in the presence of additional equivalents of THF. It seems reasonable to assume for cationic $[(Ph_2SiP_2)Pt(Me)(THF)]^+$ (**14**) that THF is competing with benzene to bind to the metal center, in accord with the THF self-exchange data acquired in benzene-$d_6$. Given that $k_{ex}$ for neutral $[Ph_2BP_2]Pt(Me)(THF)$ (**13**) shows no [THF] dependence for THF self-exchange, we interpret the [THF] dependence of the decay rate of **13** in benzene to imply that the addition of THF affects an equilibrium process preceding C−H activation which is not ligand exchange.

**III.2. Evidence for Reversible Ligand Metalation Processes Operative in the Chemistry of Neutral 13.** The solution NMR data obtained for unlabeled $[Ph_2BP_2]Pt(Me)(THF)$ (**13**) and its $^{13}C$-$CH_3$ and $d_{20}$-$[Ph_2BP_2]$-labeled derivatives $[Ph_2BP_2]Pt(^{13}CH_3)(THF)$ (**13-$^{13}$CH$_3$**) and $[Ph_2B(CH_2P(C_6D_5)_2)_2]Pt(Me)(THF)$ (**13-$d_{20}$**) allow us to suggest that reversible $[Ph_2BP_2]$ ligand metalation processes dominate the chemistry of neutral **13**. In comparison, the solution data obtained for $[(Ph_2SiP_2)Pt(Me)(THF)]^+$ (**14**) and $[(dppp)Pt(Me)(THF)]^+$ (**15**) provide no direct evidence for related processes: inspection of the $^{31}P\{^1H\}$ NMR spectrum of analytically pure **14** and **15** at 25 °C showed only a single species. Although the observation of small amounts of $CH_4$ upon thermolysis of $[(Ph_2SiP_2)Pt(Me)(THF)]^+$ (**14**) and $[(dppp)Pt(Me)(THF)]^+$ (**15**) in benzene-$d_6$ suggests the likelihood that ligand activation processes may be operative to some modest extent, they are certainly much less prevalent. For neutral $[Ph_2BP_2]Pt(Me)(THF)$ (**13**), $[Ph_2BP_2]$ metalation processes involve both the arylphosphine positions and the diphenylborate unit. Most striking is that the NMR data provides strong evidence for a spectroscopically observable platinum(IV) methyl hydride (intermediate **B**), a species that would result from metalation of the diphenylborate unit. Species such as **B** are typically not observable due to facile reductive elimination to regenerate platinum(II). The chelate structure postulated for **B** (Figure 9) is expected to be stable given the excellent chelate properties of the tris(phosphino)borate ligand $[PhBP_3]$,[32] a tripodal ligand whose chelate ring sizes compare well with those shown in **B**.

If our assignment of **B** is correct, neutral $[Ph_2BP_2]Pt(Me)(THF)$ (**13**) represents the first system in which a *reversibly formed* platinum(IV) intermediate is observable within a platinum(II) system that also mediates a well-defined, intermolecular

(32) We note that the 6-coordinate platinum(IV) complex $[PhBP_3]PtMe_3$ has been prepared and is thermally very robust. J. C. Thomas, J. C. Peters, unpublished results.

***Table 6.*** Summary of Key Mechanistic Observables for the Degradation of **13** and **14** in Benzene

| $(Ph_2SiP_2)Pt(Me)(THF)^{\oplus}$ **14** $\xrightarrow{\text{PhH or PhD}}$ $(Ph_2SiP_2)Pt(Ph)(THF)^{\oplus}$ **17** ($-CH_4$ or $CH_3D$) | $[Ph_2BP_2]Pt(Me)(THF)$ **13** $\xrightarrow{\text{PhH or PhD}}$ $[Ph_2BP_2]Pt(Ph)(THF)$ **16** ($-CH_4$ or $CH_3D$) |
|---|---|
| • rate of C−H activation at 55 °C: $k = 1.80(6) \times 10^{-4}\ s^{-1}$ | • rate of C−H activation at 45 °C: $k = 1.42(5) \times 10^{-4}\ s^{-1}$ |
| • rate of C−D activation at 55 °C: $k = 2.76(7) \times 10^{-5}\ s^{-1}$ | • rate of C−D activation at 45 °C: $k = 1.13(3) \times 10^{-4}\ s^{-1}$ |
| • $k(C_6H_6)/k(C_6D_6)$ for **14** = 6.52 at 55 °C | • $k(C_6H_6)/k(C_6D_6)$ at 45 °C for **13** = 1.26 |
| | • $k(C_6H_6)/k(C_6D_6)$ at 45 °C for **13-*d*$_{20}$** = 1.8 |
| • k**13**/k**14** in $C_6D_6$ at 55 °C is ∼14 | • k**13**/k**13-*d*$_{20}$** in $C_6D_6$ at 55 °C is ∼3.1 |
| • k**13**/k**14** in $C_6H_6$ at 55 °C is ∼2.5 | • k**13**/k**13-*d*$_{20}$** in $C_6H_6$ at 55 °C is ∼2 |
| • mechanism of THF self-exchange is associative<br>activation parameters:<br>$\Delta S^{\ddagger} = -30.2 \pm 5.2$ e.u. and<br>$\Delta H^{\ddagger} = 1.9 \pm 0.5$ kcal/mol | • mechanism of THF self-exchange is ligand-assisted (or dissociative)<br>activation parameters:<br>$\Delta S^{\ddagger} = -0.1 \pm 5.4$ e.u. and<br>$\Delta H^{\ddagger} = 16.0 \pm 1.6$ kcal/mol |
| • $CH_4$:$CH_3D$ ratio for methane byproduct after thermolysis of **14** in $C_6D_6$: 1.0:7.6 | • $CH_4$:$CH_3D$ ratio for methane byproduct after thermolysis of **13** in $C_6D_6$: 3.0:1.0 |
| | • $CH_4$:$CH_3D$ ratio for methane byproduct after thermolysis of **13-*d*$_{20}$** in $C_6D_6$: 1.0:7.3 |
| • negligible deuterium incorporation into the $(Ph_2SiP_2)$ ligand after thermolysis in benzene-$d_6$ | • significant deuterium incorporation into the $[Ph_2BP_2]$ ligand after thermolysis in benzene-$d_6$ |
| • $(Ph_2SiP_2)$ metalation in benzene solution is kinetically noncompetitive with benzene C−H activation processes | • $[Ph_2BP_2]$ metalation in benzene solution is kinetically very competitive with benzene C−H activation processes |
| • no spectroscopically observable intermediates | • several spectroscopically observable intermediates |

C−H bond activation process. Given the similarity between a $[Ph_2BP_2]$ phenyl ring substrate and benzene itself, it is quite reasonable to suggest that the intermolecular benzene activation process also proceeds via a platinum(II/IV) couple, as has been asserted for a host of related platinum(II) systems that display intermolecular C−H activation chemistry.[5−12]

It appears to be possible to inhibit ligand metalation processes prevalent in $[Ph_2BP_2]Pt(Me)(THF)$ (**13**) by turning to an L-type ligand that is more sterically encumbered. Such a comparison is provided by the solution chemistry of $[Ph_2BP_2]Pt(Me)\{P(C_6F_5)_3\}$ (**25**). Although **25** exhibits a similar benzene C−H activation reaction, thermolysis of **25** in benzene-$d_6$ gives rise to a very different ratio in the released methane isotopomers by comparison to **13**. The observed ratio for $[Ph_2BP_2]Pt(Me)\{P(C_6F_5)_3\}$ (**25**) was very similar to that observed for its cationic counterpart $[(Ph_2BP_2)Pt(Me)\{P(C_6F_5)_3\}]^+$ (**29**). To explain these data, we suggest that the steric bulk of **25** prohibits anchimeric $\eta^3$-binding of its $[Ph_2BP_2]$ ligand, thereby attenuating $[Ph_2BP_2]$ ligand metalation processes that favor the release of $CH_4$ over $CH_3D$. Worth noting is that the $^{31}P\{^1H\}$ and $^1H$ NMR spectra of **25** indicate a single solution species prior to and during thermolysis, similar to the case for $[(Ph_2SiP_2)Pt(Me)(THF)]^+$ (**14**) and $[(dppp)Pt(Me)(THF)]^+$ (**15**).

**III.3. Overall Mechanistic Summary.** The benzene solution chemistry we have observed for the neutral $[Ph_2BP_2]Pt(Me)(THF)$ (**13**) is generally comparable to that observed for its isostructural but cationic relatives $[(Ph_2SiP_2)Pt(Me)(THF)]^+$ (**14**) and $[(dppp)Pt(Me)(THF)]^+$ (**15**). Each system mediates an intermolecular benzene C−H bond activation process under a similar set of reaction conditions. The zwitterionic descriptor ascribed to $[Ph_2BP_2]Pt(Me)(THF)$ (**13**) seems to comparatively predict its overall reactivity. However, important mechanistic differences exist that can be attributed to the role that the bis(phosphine)-ligand auxiliary plays in each respective system. These mechanistic distinctions most likely reflect electronic rather than steric differences. The most relevant points to consider in a mechanistic light are summarized in Table 6 and underscore the observation that $[Ph_2BP_2]Pt(Me)(THF)$ (**13**) appears to undergo ligand metalation chemistry.

For the cationic system $[(Ph_2SiP_2)Pt(Me)(THF)]^+$ (**14**) (and by analogy $[(dppp)Pt(Me)(THF)]^+$, **15**), the neutral bis(phosphine) chelate appears to be relatively innocent with respect to the C−H activation and THF exchange chemistry studied. From the THF self-exchange data for $[(Ph_2SiP_2)Pt(Me)(THF)]^+$ (**14**), we infer that ligand substitution proceeds in a bimolecular, associative fashion. We assume that this is true for THF displacement by benzene in benzene solution, a process we could not measure directly but can reasonably deduce by comparison to the THF self-exchange data. The C−H activation processes that occur in benzene solution for **14** appear also to be predominantly intermolecular in nature. Although we cannot rule-out the possibility of reversible ligand metalation processes operative in the benzene solution chemistry of **14**—indeed, a small amount of $CH_4$ is invariably observed as a byproduct upon thermolysis of **14** in benzene-$d_6$—we suggest that any intramolecular activation processes are sufficiently dominated by intermolecular processes that it is a justifiable simplification to mechanistically focus on the latter type. In Figure 11, we outline the simplest plausible mechanism (**Path A**) by which cationic **14** undergoes intermolecular benzene activation. The outlined mechanism is consistent with our data and is generally similar to that proposed for other $L_2Pt(Me)^+$ systems that have been thoroughly described elsewhere.[5−12] Key points to note in **Path A** are that benzene coordination to the cationic platinum center is likely an associative process, and the benzene activation step is likely to be rate-determining, intimated by the large primary kinetic isotope effect that was observed for **14** ($k(C_6H_6)/k(C_6D_6) = 6.52$). Although we might favor a benzene C−H activation step for the cationic system that occurs by oxidative addition from platinum(II) to give a platinum(IV) phenyl hydride, our data is unbiased and neither supports nor refutes this hypothesis.

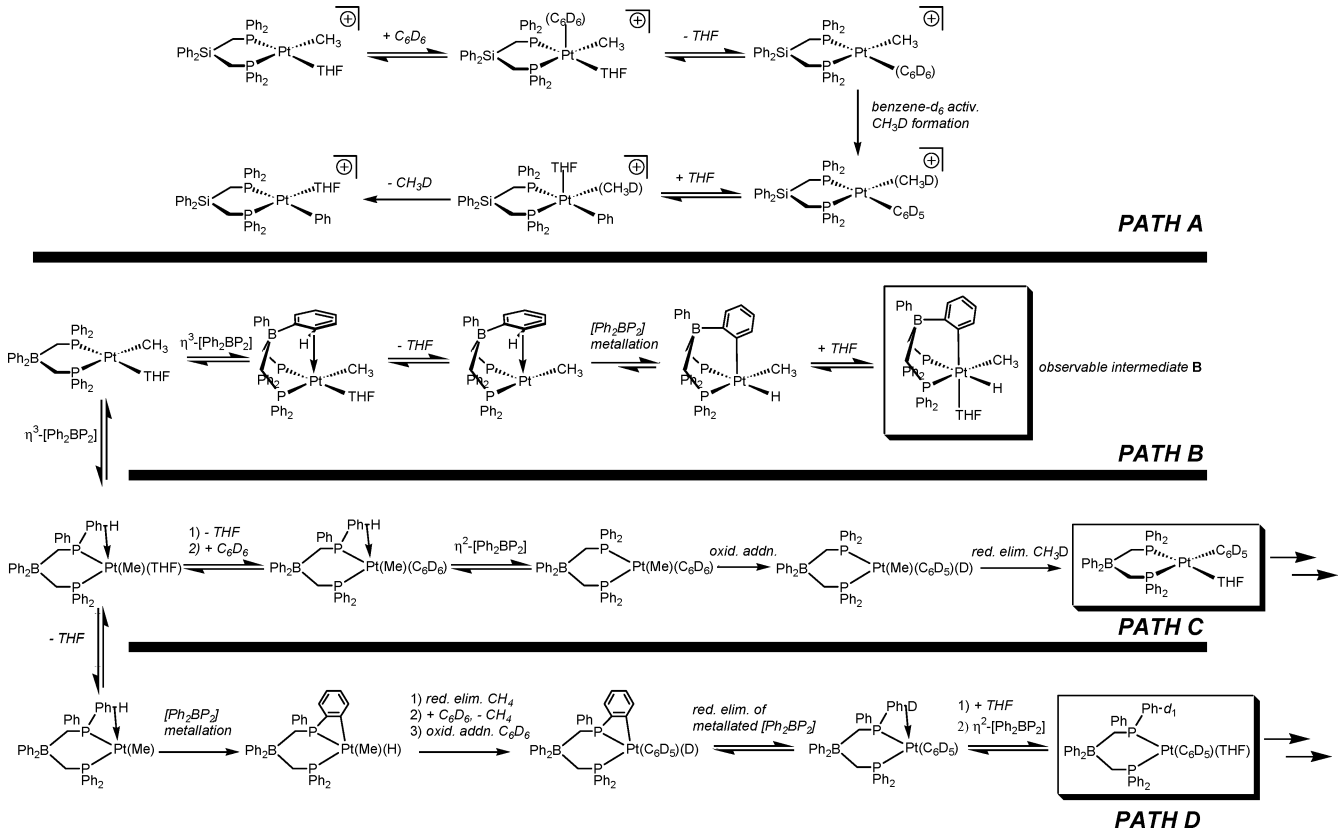


***Figure 11.*** Postulated mechanisms for the predominant pathways leading to intermolecular benzene C−H activation chemistry for cationic $[(Ph_2SiP_2)Pt(Me)(THF)]^+$ (**14**) (upper mechanism, **Path A**) and zwitterionic $[Ph_2BP_2]Pt(Me)(THF)$ (**13**) (lower mechanism, **Paths B**, **C**, and **D**).

The neutral system $[Ph_2BP_2]Pt(Me)(THF)$ (**13**) differs from $[(Ph_2SiP_2)Pt(Me)(THF)]^+$ (**14**) in that the bis(phosphine) auxiliary is intimately involved in both ligand exchange and C−H activation processes operative in benzene solution. The zero-order dependence in THF for THF self-exchange reflects the ability of the $[Ph_2BP_2]$ ligand to assist in ligand exchange by an $\eta^3$-binding mode, an intramolecular process akin to a solvent-assisted ligand substitution process. Although THF loss might also be dissociative based upon our exchange data, the prevailing ligand metalation chemistry of $[Ph_2BP_2]Pt(Me)(THF)$ (**13**) persuades us to discount this latter possibility. This propensity for the $[Ph_2BP_2]$ ligand to achieve an $\eta^3$-binding mode dramatically impacts the nature of the C−H activation processes that are observed in benzene solution.

In Figure 11, we outline three mechanistic pathways to account for the solution chemistry of $[Ph_2BP_2]Pt(Me)(THF)$ (**13**). These are labeled **Path B**, **Path C**, and **Path D**, respectively. Association of an aryl ring from the diphenylborate unit of **13** leads down **Path B** to a metalation process that generates a platinum(IV) methyl hydride complex (product **B**), an intermediate that can be spectroscopically detected. We do not think product **B** precedes an intermolecular benzene C−H activation step. Rather, we think that metalation at the diphenylborate unit is reversible and that product **B** is ultimately funneled along **Paths C** and **D**. Common to **Paths C** and **D** is an $\eta^3$-binding mode for the $[Ph_2BP_2]$ auxiliary that involves the arylphosphine donor rather than the diphenylborate unit. **Path C** proceeds along a simpler scenario that invokes a $[Ph_2BP_2]$-assisted benzene-$d_6$ substitution for THF, followed by oxidative addition of benzene-$d_6$ and reductive elimination of $CH_3D$, the methane byproduct expected. The key distinction between **Path C** and **Path A** is the mechanism by which benzene enters the platinum coordination sphere. Our intuition is to suggest that the rate-determining step along **Path C** is the C−H activation step, and that the negligible primary kinetic isotope effect that was measured for $[Ph_2BP_2]Pt(Me)(THF)$ (**13**) ($k(C_6H_6)/k(C_6D_6) = 1.26$) is due to the kinetic dominance of the fourth path, **Path D**. In this last pathway, arylphosphine ligand metalation processes occur that produce platinum(IV) methyl hydride-species distinct from product **B** (shown in **Path B**). After ligand metalation, benzene-$d_6$ enters the platinum coordination sphere at one of several indistinguishable stages, each of which involves the reductive elimination of $CH_4$ (for simplicity only one scenario is presented in Figure 11 explicitly). C−D activation of benzene-$d_6$, followed by a reverse metalation process that transfers dueteride into the $[Ph_2BP_2]$ ligand, ultimately leads to the phenyl platinum complex. **Path D** thus accounts for the high degree of $CH_4$ released by **13** in benzene-$d_6$ and the incorporation of deuteride into the $[Ph_2BP_2]$ ligand. We are comfortable explicitly invoking platinum(IV) intermediates along both **Paths C** and **D** that arise from oxidative addition of benzene-$d_6$ because of our spectroscopic evidence for a platinum(IV) species resulting from $[Ph_2BP_2]$ metalation (product **B**, **Path B**). Also, we emphasize that our inability to detect the platinum(IV) hydride species produced by $[Ph_2BP_2]$ metalation along **Path D** is because the ligand metalation process is itself rate-determining. Recall a key piece of evidence that supports this assertion—in both benzene and benzene-$d_6$, the rate of decay of the $d_{20}$-labeled derivative $[Ph_2B(CH_2P(C_6D_5)_2)_2]Pt(Me)(THF)$ (**13-*d*$_{20}$**) is *significantly* slower than that of $[Ph_2BP_2]Pt(Me)(THF)$ (**13**) itself ($k_{13}/k_{13-d20} \approx 3$ in benzene-$d_6$). Under conditions in which **Path D**

dominates and ligand metalation is rate-determining, this is just what we expect.

The observation that the rate of decay of $[Ph_2B(CH_2P(C_6D_5)_2)_2]Pt(Me)(THF)$ (**13-*d*$_{20}$**) is modestly slower in benzene-$d_6$ than in protio benzene (for **13-*d*$_{20}$**, $k(C_6H_6)/k(C_6D_6) \approx 1.8$) is perhaps more curious, but is conveniently explained as follows: deuteration of the aryl positions of the $[Ph_2BP_2]$ ligand slows the rate of ligand metalation, and thereby attenuates the overall rate by which **13-*d*$_{20}$** traverses down **Path D**. This in turn funnels more of the system down **Path C**, a path insensitive to arylphosphine deuteration. In this manner, a preequilibrium shift in benzene-$d_6$ serves to amplify the primary kinetic isotope effect of **Path C** and thereby expose C−H activation as rate-determining along this path as well. We can therefore suggest that a C−H activation process of some sort is rate-determining for each of the four distinct pathways that are outlined in Figure 11.

The final task we are left with is to account for the large role that the $[Ph_2BP_2]$ ligand plays in the solution chemistry of neutral $[Ph_2BP_2]Pt(Me)(THF)$ (**13**), whereas the $Ph_2SiP_2$ ligand appears to be far more innocent with respect to the solution chemistry of cationic $[(Ph_2SiP_2)Pt(Me)(THF)]^+$ (**14**). The key distinction between the two ligands is the propensity for the $[Ph_2BP_2]$ ligand to achieve an $\eta^3$-binding mode, a binding mode that is less prevalent for the neutral ligand $Ph_2SiP_2$. Because each ligand is sterically very similar, we commit ourselves to an electronic explanation that underscores the more electron-rich nature of **13** relative to **14**. It seems reasonable to suggest that some of the anionic borate charge is disseminated to the aryl groups of the $[Ph_2BP_2]$ ligand. This results in aryl groups in the $[Ph_2BP_2]$ ligand that are better electron-pair donors than the aryl groups of the neutral $Ph_2SiP_2$ ligand. Therefore, although benzene outcompetes the aryl donors of the $Ph_2SiP_2$ ligand with respect to coordinating platinum, thereby leading to the intermolecular solution chemistry observed, benzene does not outcompete the aryl groups of the $[Ph_2BP_2]$ ligand, and intramolecular processes become prevalent. This subtle electronic distinction might thereby have the effect of skewing the overall mechanistic bias between the neutral and cationic systems.

The propensity for a structurally related neutral and cationic platinum(II) system to mediate intermolecular benzene C−H activation is generally comparable. However, the operational mechanism by which each system mediates this chemistry is distinct. The mechanism by which substrate coordination occurs, and the propensity for intramolecular ligand C−H activation processes, is clearly different between the neutral and cationic systems. This study, along with several others,[3] now allows us to conclude that zwitterions of the type described herein are generally capable of undergoing organometallic reactions akin to their cation cousins. However, understanding the intimate mechanism by which these zwitterions mediate elementary reaction transformations will help to define a unique and complementary role for zwitterions in catalysis.

**Experimental.** Unless otherwise noted, all syntheses were carried out in the absence of water and dioxygen, using standard Schlenk and glovebox techniques. Tetrahydrofuran, diethyl ether, toluene, benzene, dichloromethane, and petroleum ether were deoxygenated and dried by thorough sparging with $N_2$ gas followed by passage through an activated alumina column. Hydrocarbon and ethereal solvents were typically tested with a standard purple solution of sodium benzophenone ketyl in tetrahydrofuran in order to confirm effective oxygen and moisture removal. Deuterated chloroform, benzene, dichloromethane, acetonitrile, and acetone were purchased from Cambridge Isotope Laboratories, Inc. and were degassed by repeated freeze−pump−thaw cycles and dried over activated 3-Å molecular sieves prior to use. $(COD)PtCl_2$,[33] (COD)PtMeCl,[33] $(COD)PtMe_2$,[34] $(COD)Pt(^{13}CH_3)_2$,[31] (COD)PtMePh,[35] $(COD)PtPh_2$,[36] $Ph_2PMe$,[37] $Ph_2PCH_2Li(TMEDA)$,[38] ASNBr,[39] $[Li(Et_2O)_2][B(C_6F_5)_4]$,[40] $[H(Et_2O)_2][B(C_6F_5)_4]$,[15] $[^nBu_4N][B(C_6F_5)_4]$,[41] $(dppp)Mo(CO)_4$,[22] $(dppp)PtMe_2$,[14b] and $P(C_6F_5)_3$[42] were prepared by previously described methods. $(dppp)PtPh_2$[16] was prepared by reaction of $(COD)PtPh_2$ with dppp in THF solution. $B(C_6F_5)_3$ was purchased from Aldrich and recrystallized from pentane at −35 °C prior to use. $[HNEt_3][BPh_4]$ was prepared by stirring an aqueous solution of $HNEt_3Cl$ and $NaBPh_4$. $[HNEt^iPr_2][BPh_4]$[43] was prepared by acidifying an aqueous solution of $NEt^iPr_2$ with HCl (aq) and adding $NaBPh_4$. The resulting white precipitate was collected by filtration and dried under heat and vacuum for 24 h prior to use. All other chemicals were purchased from commercial vendors and used without further purification. NMR spectra were recorded at ambient temperature on Varian Mercury 300 MHz and Inova 500 MHz, and Joel 400 MHz spectrometers, unless otherwise noted. $^1H$ and $^{13}C$ NMR chemical shifts were referenced to residual solvent. $^{31}P$ NMR, $^{11}B$ NMR, and $^{19}F$ NMR chemical shifts are reported relative to an external standard (0 ppm) of 85% $H_3PO_4$, neat $BF_3{\cdot}Et_2O$, and neat $CFCl_3$ respectively. IR spectra were recorded on a Bio-Rad Excalibur FTS 3000 spectrometer at 2 $cm^{-1}$ resolution controlled by Win-IR Pro software using a KBr solution cell. Elemental Analyses were performed by Desert Analytics, Tucson, AZ. X-ray diffraction experiments were carried out by the Beckmann Institute Crystallographic Facility on a Siemens CCD diffractometer.

**$[Ph_2B(CH_2PPh_2)_2][ASN]$ ($[Ph_2BP_2]$, 1).** Solid pale yellow $Ph_2PCH_2Li(TMEDA)$ (4.82 g, 15.0 mmol) was dissolved in diethyl ether (180 mL) in a Schlenk flask with a stir bar and sealed with a septum. The reaction vessel was cooled to −78 °C in a dry ice/acetone bath. $Ph_2BCl$ (1.514 g, 7.553 mmol), dissolved in toluene (10 mL), was introduced dropwise via syringe to the cooled reaction flask. The reaction was stirred and warmed gradually to r.t. over 14 h, providing a pale yellow precipitate. Volatiles were removed under reduced pressure, and the resulting solids were isolated in a drybox on a sintered glass frit and washed with diethyl ether [5 × 10 mL]. Drying under reduced pressure provided pale yellow solid $[Ph_2B(CH_2PPh_2)_2][Li(TMEDA)_2]$ (5.67 g).

Solid $[Ph_2B(CH_2PPh_2)_2][Li(TMEDA)_2]$ was dissolved in ethanol (40 mL). ASNBr (1.8 g, 8.7 mmol) was dissolved in ethanol (8 mL) and added to stirring **1**. A white precipitate

(33) Clark, H. C.; Manzer, L. E. *J. Organomet. Chem.* **1973**, *59*, 411−428.
(34) Costa, E.; Pringle, P. G.; Ravetz, M. *Inorg. Synth.* **1995**, *31*, 284−286.
(35) Hackett, M.; Whitesides, G. M. *Organometallics* **1987**, *6*, 403−410.
(36) Appleton, T. G.; Bennett, M. A. *Inorg. Chem.* **1978**, *17*, 738−747.
(37) Seyferth, D.; Burlitch, J. M. *J. Org. Chem.* **1963**, *28*, 2463.
(38) Schore, N. E.; Benner, L. S.; Labelle, B. E. *Inorg. Chem.* **1981**, *20*, 3200−3208.
(39) Blicke, F. F.; Hotelling, E. B. *J. Am. Chem. Soc.* **1954**, *76*, 5099−5103.
(40) Stehling, U. M.; Stein, K. M.; Kesti, M. R.; Waymouth, R. M. *Macromolecules* **1998**, *31*, 2019−2027.
(41) LeSuer, R. J.; Geiger, W. E. *Angew. Chem., Int. Ed.* **2000**, *39*, 248−250.
(42) Kemmitt, R. D. W.; Nichols, D. I.; Peacock, R. D. *J. Chem. Soc. A* **1968**, 2149−2152.
(43) Bakshi, P. K.; Linden, A.; Vincent, B. R.; Roe, S. P.; Adhikesavalu, D.; Cameron, T. S.; Knop, O. *Can. J. Chem.* **1994**, *72*, 1273−1293.

formed immediately. The mixture was stirred for 10 min, and white solids were subsequently collected by filtration. The solids were washed with ethanol [2 × 10 mL] and diethyl ether [3 × 10 mL] and dried under reduced pressure for 24 h, providing **1** as a pure, white solid (4.30 g, 6.23 mmol, 83.1%).

$^1$H NMR (300 MHz, acetone-$d_6$): $\delta$ 7.29 (br, 4H, *ortho* B($C_6H_5$)$_2$), 7.17 (m, 8H, *ortho* P($C_6H_5$)$_2$), 7.00 (m, 12H, *meta* B($C_6H_5$)$_2$ and P($C_6H_5$)$_2$), 6.74 (m, 4H, *para* P($C_6H_5$)$_2$), 6.62 (m, 2H, *para* B($C_6H_5$)$_2$), 3.65 (m, 8H, (($CH_2CH_2$)$_2$)$_2$N), 2.23 (m, 8H, (($CH_2CH_2$)$_2$)$_2$N), 1.64 (br, 4H, $Ph_2B(CH_2PPh_2)_2$). $^{13}$C{$^1$H} NMR (125.7 MHz, acetone-$d_6$): $\delta$ 165 (br, *ipso* B($C_6H_5$)$_2$), 147.4 (d, *ipso* P($C_6H_5$)$_2$, $^1J_{P-C}$ = 22 Hz), 134.7 (s, *ortho* B($C_6H_5$)$_2$), 133.6 (d, *ortho* P($C_6H_5$)$_2$, $^2J_{P-C}$ = 19 Hz), 127.1 (s, *meta* P($C_6H_5$)$_2$, $^3J_{P-C}$ = 6 Hz), 126.0 (s, *para* P($C_6H_5$)$_2$), 125.3 (s, *meta* B($C_6H_5$)$_2$), 121.5 (s, *para* B($C_6H_5$)$_2$), 63.1 ((($CH_2CH_2$)$_2$)$_2$N), 25.7 (br, [$Ph_2B(CH_2PPh_2)_2$]), 22.1 ((($CH_2CH_2$)$_2$)$_2$N). $^{31}$P{$^1$H} NMR (121.4 MHz, acetone-$d_6$): $\delta$ −8.78 ($^2J_{P-B}$ = 10.0 Hz). $^{11}$B{$^1$H} NMR (128.3 MHz, acetone-$d_6$): $\delta$ −12.6. Anal. Calcd. for $C_{46}H_{50}BNP_2$: C, 80.11; H, 7.31; N, 2.03. Found: C, 79.89; H, 7.45; N, 2.15.

**($C_6H_5$)$_2$Si($CH_2PPh_2$)$_2$ ($Ph_2SiP_2$, 2).** Solid pale yellow $Ph_2PCH_2Li$(TMEDA) (7.1300 g, 22.119 mmol) was suspended in diethyl ether (100 mL) in a 250 mL Schlenk flask with a stirbar and a septum. The flask was cooled to −78 °C in a dry ice/acetone bath. Separately, diphenyldichlorosilane (2.7981 g, 11.051 mmol) was dissolved in diethyl ether (10 mL) and was transferred by syringe to the cold reaction flask. The mixture was allowed to stir and warm gradually over 7 h. Volatiles were removed under reduced pressure, and the resulting solids were collected on a sintered glass frit and washed with diethyl ether [3 × 10 mL], removing yellow impurities and leaving white solids. The solids were dissolved in dichloromethane (50 mL), and the hazy solution was filtered over Celite on a sintered glass frit. Volatiles were removed under reduced pressure from the resulting clear, colorless solution, providing white solid $Ph_2Si(CH_2PPh_2)_2$ (5.2838 g, 82.3%).

$^1$H NMR (300 MHz, $C_6D_6$): $\delta$ 7.46 (dd, 4H), 7.31 (m, 8H), 7.05 (m, 6H), 6.97 (m, 12H), 1.89 (s, 4H, $Ph_2Si(CH_2PPh_2)_2$). $^{13}$C{$^1$H} NMR (125.7 MHz, $C_6D_6$): $\delta$ 141.6, 136.0, 133.3, 129.8, 128.8, 128.2, 116.7, 12.4 (dd, $Ph_2Si(CH_2PPh_2)_2$, $J$ = 33 Hz, $J$ = 4.8 Hz). $^{31}$P{$^1$H} NMR (121.4 MHz, $C_6D_6$): $\delta$ −23.29. $^{31}$P{$^1$H} NMR (121.4 MHz, acetone-$d_6$): $\delta$ −22.65. $^{29}$Si{$^1$H} NMR (99.3 MHz, THF): $\delta$ −10.42 (t, $^2J_{Si-P}$ = 17.0 Hz). Anal. Calcd. for $C_{38}H_{34}P_2Si$: C, 78.59; H, 5.90. Found: C, 78.89; H, 5.78.

**[[$Ph_2BP_2$]Mo(CO)$_4$][ASN] (4).** Solid Mo(CO)$_6$ (53.4 mg, 202 $\mu$mol) and solid [$Ph_2BP_2$][ASN] (133.0 mg, 192.8 $\mu$mol) were combined and dissolved in THF (3 mL). The sealed vessel was placed under partial vacuum and heated to 65 °C for 36 h. The resulting pale yellow solution was cooled to r.t., and volatiles were removed under reduced pressure. The pale yellow solids were washed with petroleum ether [3 × 2 mL] and dried under reduced pressure, providing analytically pure [[$Ph_2BP_2$]Mo(CO)$_4$][ASN] (168.5 mg, 97.3%).

$^1$H NMR (300 MHz, $CD_3CN$): $\delta$ 7.36 (m, 8H), 7.11 (m, 12H), 6.94 (br d, 4H), 6.69 (m, 4H), 6.61 (m, 2H), 3.37 (m, 8H), 2.11 (m, 8H), 1.98 (br, 4H). $^{13}$C{$^1$H} NMR (75.4 MHz, $CD_3CN$): $\delta$ 220.0 (m), 213.6 (m), 166 (br), 143.6 (m), 133.6, 133.0 (m), 128.6, 128.1, 126.6, 122.6, 63.8, 23.9 (br), 22.7. $^{31}$P{$^1$H} NMR (121.4 MHz, $CD_3CN$): $\delta$ 29.37. $^{11}$B{$^1$H} NMR (128.3 MHz, $CD_3CN$): $\delta$ −14.1. IR: ($CH_2Cl_2$) $\nu_{CO}$ = 2005, 1896, 1849 cm$^{-1}$. Anal. Calcd. for $C_{50}H_{50}BMoNO_4P_2$: C, 66.90; H, 5.61; N, 1.56. Found: C, 67.04; H, 5.82; N, 1.52.

**($Ph_2SiP_2$)Mo(CO)$_4$ (5).** Solid Mo(CO)$_6$ (50.3 mg, 191 $\mu$mol) and solid $Ph_2Si(CH_2PPh_2)_2$ (108.2 mg, 186.3 $\mu$mol) were combined and dissolved in THF (3 mL). The sealed vessel was placed under partial vacuum and heated to 65 °C for 36 h. The resulting colorless solution was cooled to r.t., and volatiles were removed under reduced pressure. The off-white solids were washed with petroleum ether [3 × 2 mL] and dried under reduced pressure, providing analytically pure ($Ph_2SiP_2$)Mo(CO)$_4$ (139.5 mg, 95.0%).

$^1$H NMR (300 MHz, $CDCl_3$): $\delta$ 7.46 (m, 8H), 7.26 (m, 12H), 7.21 (m, 2H), 7.05 (t, 4H, $J_{H-H}$ = 7.8 Hz), 6.95 (dd, 4H, $J_{H-H}$ = 1.5, 7.8 Hz), 2.29 (d, 4H, $J_{P-H}$ = 7.8 Hz). $^{13}$C{$^1$H} NMR (75.4 MHz, $CDCl_3$): $\delta$ 215.4 (dd, $J_{P-C}$ = 7.6, 7.6 Hz), 210.8 (t, $J_{P-C}$ = 8.5 Hz), 139.3 (m), 134.6 (m), 134.3, 131.9 (m), 129.6, 129.5, 128.4 (m), 127.9, 13.6 (m). $^{31}$P{$^1$H} NMR (121.4 MHz, $CDCl_3$): $\delta$ 23.50. IR: ($CH_2Cl_2$) $\nu_{CO}$ = 2018, 1922, 1896 cm$^{-1}$. Anal. Calcd. for $C_{42}H_{34}MoO_4P_2Si$: C, 63.96; H, 4.35. Found: C, 64.15; H, 4.09.

**[[$Ph_2BP_2$]Pt(Me)$_2$][ASN] (7).** Solid [$Ph_2BP_2$][ASN] (391.8 mg, 0.5680 mmol) was suspended in THF (6 mL). A solution of (COD)Pt(Me)$_2$ (189.3 mg, 0.5679 mmol) in THF (2 mL) was added to the suspension, and the reaction homogenized as it stirred. A white precipitate formed after 1 h. The resulting mixture was concentrated under reduced pressure and triturated with pentane [2 × 2 mL]. The off white solids were dried under reduced pressure, providing **7** as an off-white solid (511.2 mg, 98.4%). Crystals suitable for X-ray diffraction were grown from slow evaporation of an acetonitrile solution of **7**.

$^1$H NMR (300 MHz, acetone-$d_6$): $\delta$ 7.40 (m, 8H), 7.07 (m, 12H), 6.88 (m, 4H), 6.64 (m, 4H), 6.58 (m, 2H), 3.71 (m, 8H), 2.26 (m, 8H), 1.98 (br, 4H), 0.08 (t, 6H, $^3J_{P-H}$ = 12 Hz, $^2J_{Pt-H}$ = 68 Hz). $^{13}$C{$^1$H} NMR (125.7 MHz, acetone-$d_6$): $\delta$ 167 (br), 140.1 (d), 134.4 (m), 133.5, 128.2, 127.3 (m), 126.3 (m), 122.0, 63.7, 22.9 (br), 22.8, 5.5 (dd, $^1J_{Pt-C}$ = 600 Hz, $^2J_{P-C}$ = 103 Hz, $^2J_{P-C}$ = 9.1 Hz). $^{31}$P{$^1$H} NMR (121.4 MHz, acetone-$d_6$): $\delta$ 20.60 ($^1J_{Pt-P}$ = 1892 Hz). $^{11}$B{$^1$H} NMR (128.3 MHz, acetone-$d_6$): $\delta$ −13.7. Anal. Calcd. for $C_{48}H_{56}BNP_2Pt$: C, 63.02; H, 6.17; N, 1.53. Found: C, 62.97; H, 5.90; N, 1.81.

**($Ph_2SiP_2$)PtMe$_2$ (8).** Solid **2** (199.7 mg, 0.3439 mmol) and CODPtMe$_2$ (114.4 mg, 0.3432 mmol) were dissolved in THF (4 mL). After 30 min, volatiles were removed under reduced pressure. The resulting solids were triturated with petroleum ether (4 mL), and the solution was decanted. The resulting off-white solids were dried under reduced pressure, providing **8** (253.9 mg, 91.6%). Crystals suitable for X-ray diffraction were grown from petroleum ether vapor diffusion into a toluene solution of **8**.

$^1$H NMR (300 MHz, $CDCl_3$): $\delta$ 7.52 (m, 8H), 7.2−7.3 (m, 14H), 7.06 (t, 4H), 6.95 (dd, 4H), 2.29 (d, 4H, $^2J_{P-H}$ = 9.9 Hz, $^3J_{Pt-H}$ = 25 Hz), 0.31 (dd, 6H, $^3J_{P-H}$ = 6.3, 8.7 Hz, $^2J_{Pt-H}$ = 68 Hz). $^1$H NMR (300 MHz, acetone-$d_6$): $\delta$ 7.56 (m, 8H), 7.2−7.3 (m, 14H), 7.08 (m, 8H), 2.41 (d, 4H, $^2J_{P-H}$ = 9.9 Hz, $^3J_{Pt-H}$ = 25 Hz), 0.17 (dd, 6H, $^3J_{P-H}$ = 6.6, 8.1 Hz, $^2J_{Pt-H}$ = 69 Hz). $^{13}$C{$^1$H} NMR (125.7 MHz, $CDCl_3$): $\delta$ 135.4 (m), 134.9 (m), 134.1 (s), 133.5 (m), 129.8 (s), 129.4 (s), 127.9 (m), 127.9 (s), 10.5 (m), 5.7 (dd, 6H, $^2J_{P-C}$ = 7.9, 101 Hz, $^1J_{Pt-C}$ = 596 Hz). $^{31}$P{$^1$H} NMR (121.4 MHz, $CDCl_3$): $\delta$ 14.35 ($^1J_{Pt-P}$ = 1822

Hz). $^{31}P\{^1H\}$ NMR (121.4 MHz, acetone-$d_6$): $\delta$ 12.00 ($^1J_{Pt-P}$ = 1848 Hz). $^{29}Si\{^1H\}$ NMR (99.3 MHz, THF): $\delta$ −13.57. Anal. Calcd. for $C_{40}H_{40}P_2PtSi$: C, 59.62; H, 5.00. Found: C, 59.36; H, 5.07.

**[Ph$_2$BP$_2$]Pt(Me)(CO) (10).** A THF solution (2 mL) of [Et$_3$NH][BPh$_4$] (47.5 mg, 0.113 mmol) was added to a stirring THF solution (15 mL) of **7** (103.3 mg, 0.1129 mmol). Formation of a white precipitate occurred gradually over 15 min. The reaction was filtered, removing the white solids, and the solution was transferred to a 50 mL Schlenk flask and sealed with a septum and a needle valve. A stream of CO was passed through the flask for 5 min. The septum was exchanged for a stopper under an N$_2$ flow, and the volatiles were removed under reduced pressure. The resulting solids were dissolved in THF (10 mL), filtered, concentrated, triturated with pentane [2 × 2 mL], washed with Et$_2$O [3 × 2 mL], and dried under reduced pressure, providing **10** (78.1 mg, 86.3%).

$^1H$ NMR (300 MHz, CDCl$_3$): $\delta$ 7.12−7.34, 6.85−6.92, 6.72−6.83 (aryl protons), 2.14 (br, 2H, $^3J_{Pt-H}$ = 61 Hz), 2.09 (br, 2H, $^3J_{Pt-H}$ = 54 Hz), 0.45 (t, 3H, $^2J_{Pt-H}$ = 58 Hz, $^3J_{Pt-P}$ = 6.0 Hz). $^{13}C\{^1H\}$ NMR (125.7 MHz, CDCl$_3$): $\delta$ 180.5 (dd, Pt-*C*O, $^1J_{Pt-C}$ = 1291 Hz, $^2J_{P(trans)-C}$ = 131 Hz, $^2J_{P(cis)-C}$ = 6.9 Hz), 162 (br), 136.2 (d), 133.5 (d), 132.5 (d), 132.3, 131.2 (d), 130.5 (d), 130.1 (d), 128.4 (d), 128.2 (d), 126.6, 122.8, 18.2 (br), 16.4 (br), −2.6 (d, $^2J_{P-C}$ = 60 Hz). $^{31}P\{^1H\}$ NMR (121.4 MHz, CDCl$_3$): $\delta$ 20.15 (d, $^1J_{Pt-P}$ = 3053 Hz, $^2J_{P-P}$ = 31 Hz), 15.53 (d, $^1J_{Pt-P}$ = 1637 Hz, $^2J_{P-P}$ = 31 Hz). $^{11}B\{^1H\}$ NMR (160.4 MHz, CDCl$_3$): $\delta$ −14.2. IR: (Nujol mull) $\nu_{CO}$ = 2087 cm$^{-1}$. IR: (CH$_2$Cl$_2$) $\nu_{CO}$ = 2094 cm$^{-1}$. Anal. Calcd. for $C_{40}H_{37}BOP_2Pt$: C, 59.94; H, 4.65. Found: C, 60.37; H, 5.27.

**[(Ph$_2$SiP$_2$)Pt(Me)(CO)][B(C$_6$F$_5$)$_4$] (11).** Solid off-white [(Ph$_2$SiP$_2$)Pt(Me)(THF)][B(C$_6$F$_5$)$_4$] (48.2 mg, 31.3 $\mu$mol) was dissolved in dichloromethane (5 mL) in a round-bottom flask containing a stirbar and sealed with a septum. The flask was purged with carbon monoxide gas for 5 min, and allowed to stir for 1 h under carbon monoxide. The flask was dried under a stream of dinitrogen. The resulting film was triturated and washed with petroleum ether [2 × 2 mL] and dried under reduced pressure, providing [(Ph$_2$SiP$_2$)Pt(Me)(CO)][B(C$_6$F$_5$)$_4$] as a white solid (43.4 mg, 92.6%).

$^1H$ NMR (300 MHz, CD$_2$Cl$_2$): $\delta$ 7.28−7.52 (m, 22H, aryl H), 7.11 (t, 4H, $J$ = 7.5 Hz), 6.91 (d, 4H, $J$ = 6.9 Hz), 2.51 (d, 2H, $J_{P-H}$ = 14.1 Hz, $J_{Pt-H}$ = 28.2 Hz), 2.43 (dd, 2H, $J$ = 3.3 Hz, $J_{P-H}$ = 15.3 Hz, $J_{Pt-H}$ = 46.2 Hz), 0.62 (dd, 3H, $J_{P-H}$ = 6.0 Hz, $J_{Pt-H}$ = 56.4 Hz). $^{13}C\{^1H\}$ NMR (75.4 MHz, CD$_2$Cl$_2$): $\delta$ 177.5 (dd, $J_{P-C}$ = 137.9 Hz, $J_{P-C}$ = 8.2 Hz), 148.7 (d), 138.8 (d), 136.9 (d), 134.0, 133.8 (d), 133.2 (d), 132.6 (m), 132.5 (m), 131.0, 130.0 (d), 129.8 (d), 128.9, 127.5 (m), 126.7 (m), 9.2 (m), 7.2 (m), −1.2 (dd, $J_{P-C}$ = 61.6 Hz, $J_{P-C}$ = 5.2 Hz, $J_{Pt-C}$ = 400 Hz). $^{31}P\{^1H\}$ NMR (121.4 MHz, CD$_2$Cl$_2$): $\delta$ 10.31 (d, $J_{P-P}$ = 29.3 Hz, $J_{P-Pt}$ = 3238 Hz), 7.16 (d, $J_{P-P}$ = 29.3 Hz, $J_{P-Pt}$ = 1665 Hz). $^{11}B\{^1H\}$ NMR (128.3 MHz, CD$_2$Cl$_2$): $\delta$ −16.9. $^{19}F\{^1H\}$ NMR (282.1 MHz, CD$_2$Cl$_2$): $\delta$ −133.5, −163.9 (t), −167.7. IR: (CH$_2$Cl$_2$) $\nu_{CO}$ = 2118 cm$^{-1}$. Anal. Calcd. for $C_{64}H_{37}BF_{20}OP_2PtSi$: C, 51.32; H, 2.49. Found: C, 51.44; H, 2.26.

**[(dppp)Pt(Me)(CO)][B(C$_6$F$_5$)$_4$] (12).** Solid off-white [(dppp)-Pt(Me)(THF)][B(C$_6$F$_5$)$_4$] (54.0 mg, 39.3 $\mu$mol) was dissolved in dichloromethane (2 mL) in a round-bottom flask containing a stirbar and sealed with a septum. The flask was purged with carbon monoxide gas for 15 min, and subsequently dried under reduced pressure. The resulting film was triturated with petroleum ether (2 mL) and dried under reduced pressure, providing [(dppp)Pt(Me)(CO)][B(C$_6$F$_5$)$_4$] as a white solid (50.2 mg, 96.0%).

$^1H$ NMR (300 MHz, CDCl$_3$): $\delta$ 7.30−7.65 (20H, aryl protons), 2.69 (m, 4H), 2.17 (m, 2H), 0.76 ("t", $^3J_{P-H}$ = 6.00 Hz, $^2J_{Pt-H}$ = 57.3 Hz). $^{13}C\{^1H\}$ NMR (75.4 MHz, CDCl$_3$): $\delta$ 176.9 (dd, Pt-*C*O, $J_{P-C}$ = 134.0 Hz, $J_{P-C}$ = 8.6 Hz, $J_{Pt-C}$ = 1320 Hz), 150.0, 146.8, 140.0, 138.1, 136.7, 134.8, 133.2, 132.7, 132.3, 129.9, 124.8, 124.0, 24.6, 24.1, 18.8, −0.9 (dd, Pt-*C*H$_3$, $J_{P-C}$ = 59.8 Hz, $J_{P-C}$ = 4.6 Hz, $J_{Pt-C}$ = 396 Hz). $^{19}F\{^1H\}$ NMR (282 MHz, CDCl$_3$): $\delta$ −132.9 (d), −163.2 (t), −166.9 (t). $^{31}P\{^1H\}$ NMR (121.4 MHz, CDCl$_3$): $\delta$ 2.32 (d, $J_{P-P}$ = 34.8 Hz, $J_{Pt-P}$ = 3126 Hz), −4.88 (d, $J_{P-P}$ = 34.8 Hz, $J_{Pt-P}$ = 1547 Hz). $^{11}B\{^1H\}$ NMR (128.3 MHz, CDCl$_3$): $\delta$ −17.1. IR: (CH$_2$Cl$_2$) $\nu_{CO}$ = 2118 cm$^{-1}$. Anal. Calcd. for $C_{53}H_{29}BF_{20}OP_2$-Pt: C, 47.88; H, 2.20. Found: C, 47.89; H, 1.99.

**[Ph$_2$BP$_2$]Pt(Me)(THF) (13).** Solid **7** (49.3 mg, 53.9 $\mu$mol) was dissolved in THF (2 mL). A THF solution (1 mL) of [$^i$Pr$_2$EtNH][BPh$_4$] (24.3 mg, 54.1 $\mu$mol) was added to the stirring solution of **7**. The clear, colorless reaction rapidly produced a white precipitate. The mixture was stirred for 15 min, and the white solids (ASNBPh$_4$) were filtered away. The solution was concentrated under reduced pressure, and pentane (2 mL) was added, precipitating solid **13** as a spectroscopically pure solid. The solid was collected by filtration and washed with petroleum ether [2 × 4 mL]. The collected solid was dried under a stream of dry gas (dinitrogen or argon). Crystals suitable for X-ray diffraction were grown from THF at −35 °C.

$^1H$ NMR (300 MHz, C$_6$D$_6$): $\delta$ 7.64 (m, 4H), 7.48 (m, 4H), 7.24 (m, 4H), 7.00 (m, 18H), 2.90 (br, 4H), 2.51 (d, 2H, $^2J_{P-H}$ = 18 Hz), 2.37 (d, 2H, $^2J_{P-H}$ = 14 Hz), 0.71 (br, 4H), 0.35 (br d, 3H, Pt−C*H*$_3$, $^3J_{P-H}$ = 6 Hz, $^2J_{Pt-H}$ = 40 Hz). $^{13}C\{^1H\}$ NMR (125.7 MHz, THF, −5 °C): $\delta$ 160.3 (br), 134.1 (d), 130.9 (d), 130.8 (d), 130.1 (d), 129.7, 127.3, 126.9, 125.5 (d), 125.1 (d), 123.5, 119.2, 64.9, 22.6, 21.2 (br), 15.3 (br), 8.2 (dd, Pt-*C*H$_3$, $^2J_{P-C(trans)}$ = 85.5 Hz, $^2J_{P-C(cis)}$ = 4.8 Hz). $^{31}P\{^1H\}$ NMR (121.4 MHz, THF): $\delta$ 33.44 (d, $^1J_{Pt-P}$ = 1820 Hz, $^2J_{P-P}$ = 22 Hz), 15.96 (d, $^1J_{Pt-P}$ = 4478 Hz, $^2J_{P-P}$ = 22 Hz). $^{31}P\{^1H\}$ NMR (121.4 MHz, C$_6$D$_6$): $\delta$ 34.14 (d, $^1J_{Pt-P}$ = 1813 Hz, $^2J_{P-P}$ = 21 Hz), 16.09 (d, $^1J_{Pt-P}$ = 4453 Hz, $^2J_{P-P}$ = 21 Hz). $^{11}B\{^1H\}$ NMR (128.3 MHz, THF): $\delta$ −14.5. Anal. Calcd. for $C_{43}H_{45}BOP_2Pt$: C, 61.07; H, 5.36. Found: C, 61.14; H, 5.32.

**[(Ph$_2$SiP$_2$)Pt(Me)(THF)][B(C$_6$F$_5$)$_4$] (14).** Solid white (Ph$_2$SiP$_2$)-PtMe$_2$ (320.0 mg, 397.1 $\mu$mol) was dissolved in dichloromethane (2 mL) with THF (0.5 mL). Separately, [H(Et$_2$O)$_2$]-[B(C$_6$F$_5$)$_4$] (324.9 mg, 397.0 $\mu$mol) was dissolved in dichloromethane (3 mL) and added slowly to the stirring solution of (Ph$_2$SiP$_2$)PtMe$_2$, evolving gas. After addition was complete, the reaction was stirred for 10 min. Volatiles were removed under reduced pressure, and the mixture was triturated and washed with petroleum ether [2 × 2 mL]. The resulting white solids were dried under reduced pressure, providing off-white **14** (574.2 mg, 93.8%).

$^1H$ NMR (300 MHz, C$_6$D$_6$): $\delta$ 7.31 (m, 4H), 7.20 (m, 4H), 7.04 (m, 6H), 6.96 (m, 8H), 6.87 (t, 4H, $J$ = 7.6 Hz), 6.63 (d, 4H, $J$ = 6.7 Hz), 2.91 (m, 4H), 2.07 (d, 2H, $J$ = 2.4 Hz), 1.19 (d, 4H, $J$ = 12.2 Hz), 0.81 (m, 4H), 0.32 (dd, 3H, $J_{P-H}$ = 1.8, 7.3 Hz, $J_{Pt-H}$ = 41.5 Hz). $^{13}C\{^1H\}$ NMR (125.7 MHz, C$_6$D$_6$): $\delta$ 150.2, 148.3, 140.0, 138.1, 136.2, 133.7, 132.9 (m), 132.1,

132.0, 131.7, 131.6, 130.1, 129.0 (d), 128.7 (d), 127.5, 125.2 (br), 72.3, 24.4, 12.1 (dd, $J_{Pt-C}$ = 903 Hz, $J_{P-C}$ = 59 Hz, $J_{P-C}$ = 11 Hz), 11.6 (m), 7.3 (m). $^{31}P\{^1H\}$ NMR (121.4 MHz, $C_6D_6$): $\delta$ 26.48 (d, $^1J_{Pt-P}$ = 1808 Hz, $^2J_{P-P}$ = 15.9 Hz), 5.09 (d, $^1J_{Pt-P}$ = 4694 Hz, $^2J_{P-P}$ = 15.9 Hz). $^{19}F\{^1H\}$ NMR (282.1 MHz, $C_6D_6$): $\delta$ −132.2, −162.9 (t, $J$ = 21.4 Hz), −166.5 (t, $J$ = 17.1 Hz). Anal. Calcd. for $C_{67}H_{45}BF_{20}OP_2PtSi$: C, 52.19; H, 2.94. Found: C, 53.52; H, 2.91.

**[(dppp)Pt(Me)(THF)][B($C_6F_5$)$_4$] (15).** Solid (dppp)$PtMe_2$ (155.1 mg, 243.3 $\mu$mol) was dissolved in dichloromethane (1 mL) with THF (0.5 mL). Separately, [H($Et_2O$)$_2$][B($C_6F_5$)$_4$] (199.0 mg, 243.2 $\mu$mol) was dissolved in dichloromethane (3 mL) and added slowly to the stirring solution of (dppp)$PtMe_2$, evolving gas. After addition was complete, the reaction was stirred for 10 min. Volatiles were removed under reduced pressure, and the mixture was triturated and washed with petroleum ether [2 × 2 mL]. The resulting white solids were dried under reduced pressure, providing analytically pure **15** (323.1 mg, 96.7%).

$^1H$ NMR (500 MHz, $CD_2Cl_2$): $\delta$ 7.30−7.65 (20H, aryl protons), 2.65 (4H, m), 1.92 (2H, m), 1.28 (2H, m), 0.86 (2H, m), 0.42 (3H, dd, Pt−$CH_3$, $^3J_{P-H}$ = 1.50, 7.00 Hz, $^2J_{Pt-H}$ = 38.0 Hz). $^{13}C\{^1H\}$ NMR (125.7 MHz, $CD_2Cl_2$): $\delta$ 149.7, 147.8, 139.8, 137.8, 135.9, 133.4 (br m), 132.6 (br m), 129.7 (br m), 127.9, 127.4, 125.0 (br m), 73.3 ($J_{Pt-C}$ = 96 Hz), 26.9, 25.3, 19.0, 13.4 (dd). $^{31}P\{^1H\}$ NMR (121.4 MHz, $CD_2Cl_2$): $\delta$ 17.25 (d, $^1J_{Pt-P}$ = 1680 Hz, $^2J_{P-P}$ = 23.2 Hz), 2.28 (d, $^1J_{Pt-P}$ = 4550 Hz, $^2J_{P-P}$ = 23.2 Hz). $^{19}F\{^1H\}$ NMR (282 MHz, $CD_2Cl_2$): $\delta$ −133.6, −164.0 (t), −167.8. $^{11}B\{^1H\}$ NMR (128.3 MHz, $CD_2Cl_2$): $\delta$ −17.2. Anal. Calcd. for $C_{56}H_{37}BF_{20}OP_2Pt$: C, 48.96; H, 2.71. Found: C, 49.36; H, 2.77.

**[$Ph_2BP_2$]Pt(Ph)(THF) (16)** (a) Solid [[$Ph_2BP_2$]Pt(Me)(Ph)]-[ASN] (23.6 mg, 24.2 $\mu$mol) was dissolved in THF (2 mL). While stirring, solid B($C_6F_5$)$_3$ (12.5 mg, 24.4 $\mu$mol) was added. After 10 min, $^{31}P$ NMR analysis showed the formation of one major product, consistent with the formulation of **16** (see b).

(b) Solid [[$Ph_2BP_2$]Pt(Me)(Ph)][ASN] (51.4 mg, 52.6 $\mu$mol) was dissolved in THF (2 mL). A THF solution (2 mL) of [$^iPr_2EtNH$][$BPh_4$] (23.5 mg, 52.3 $\mu$mol) was added to the stirring solution. The clear, colorless reaction slowly produced a white precipitate. The mixture was stirred for 1 h, and the white solids were filtered away. The solution was concentrated under reduced pressure, and pentane (2 mL) was added, precipitating white solids. The solids were collected by filtration. NMR analysis of the solids was consistent with the formulation of **16** as the major product (∼80%). Due to the lability of the coordinated THF molecule, obtaining satisfactory combustion analysis was problematic.

$^1H$ NMR (300 MHz, $C_6D_6$): $\delta$ 7.56 (m, 4H), 7.46 (m, 4H), 7.21 (m, 4H), 6.95 (m, 18H), 6.88 (m, 2H), 6.78 (m, 2H), 6.73 (m, 1H), 2.87 (br, 4H), 2.64 (d, 2H, $^2J_{P-H}$ = 17 Hz), 2.42 (d, 2H, $^2J_{P-H}$ = 14 Hz), 0.46 (br, 4H). $^{13}C\{^1H\}$ NMR (125.7 MHz, THF): $\delta$ 161 (br), 136.3, 135.4 (d), 133.0 (d), 132.9 (d), 132.1 (d), 131.5, 129.2, 129.1, 127.6 (d), 126.9 (d), 126.4 (d), 125.5, 122.6, 121.2, 67, 26, 21 (br), 17 (br). $^{31}P\{^1H\}$ NMR (121.4 MHz, THF): $\delta$ 28.60 (d, $^1J_{Pt-P}$ = 1740 Hz, $^2J_{P-P}$ = 23 Hz), 11.20 (d, $^1J_{Pt-P}$ = 4393 Hz, $^2J_{P-P}$ = 23 Hz). $^{11}B\{^1H\}$ NMR (128.3 MHz, THF): $\delta$ −14.9.

**[($Ph_2SiP_2$)Pt(Ph)(THF)][B($C_6F_5$)$_4$] (17).** Solid white ($Ph_2SiP_2$)-$PtPh_2$ (29.3 mg, 31.5 $\mu$mol) was dissolved in dichloromethane (2 mL) with THF (0.5 mL). Separately, [H($Et_2O$)$_2$][B($C_6F_5$)$_4$] (25.8 mg, 31.5 $\mu$mol) was dissolved in dichloromethane (2 mL) and added slowly to the stirring solution of ($Ph_2SiP_2$)$PtPh_2$. After addition was complete, the reaction was stirred for 10 min. Volatiles were removed under reduced pressure, and the mixture was triturated and washed with petroleum ether [2 × 2 mL]. The resulting white solids were dried under reduced pressure, providing off-white **17** (49.2 mg, 97.4%).

$^1H$ NMR (500 MHz, $CD_2Cl_2$): $\delta$ 6.4−7.8 (aryl protons), 3.24 (4H, m), 2.58 (2H, dd, $J_{P-H}$ = 3.0, 15.5 Hz, $J_{Pt-H}$ = 80 Hz), 2.43 (2H, dd, $J_{P-H}$ = 12.5 Hz, $J_{Pt-H}$ = 94 Hz), 1.15 (4H, m). $^{13}C\{^1H\}$ NMR (125.7 MHz, $CD_2Cl_2$): $\delta$ 159 (d), 149.7, 147.8, 139.8, 137.9, 135.8, 128−134, 125.0, 124.3, 68.9, 24.5, 12.1 (m), 8.3 (m). $^{31}P\{^1H\}$ NMR (121.4 MHz, $CD_2Cl_2$): $\delta$ 21.0 (d, $J_{P-P}$ = 17.1 Hz, $J_{Pt-P}$ = 1746 Hz), 0.2 (d, $J_{P-P}$ = 17.1 Hz, $J_{Pt-P}$ = 4645 Hz). $^{19}F\{^1H\}$ NMR (282 MHz, $CD_2Cl_2$): $\delta$ −133.5, −163.9, −167.7. $^{11}B\{^1H\}$ NMR (128 MHz, $CD_2Cl_2$): $\delta$ −18.4. Anal. Calcd. for $C_{72}H_{47}BF_{20}OP_2PtSi$: C, 53.91; H, 2.95. Found: C, 53.55; H, 3.26.

**[(dppp)Pt(Ph)(THF)][B($C_6F_5$)$_4$] (18).** Solid white (dppp)-$PtPh_2$ (32.1 mg, 42.1 $\mu$mol) was dissolved in dichloromethane (2 mL) with THF (0.5 mL). Separately, [H($Et_2O$)$_2$][B($C_6F_5$)$_4$] (34.5 mg, 42.2 $\mu$mol) was dissolved in dichloromethane (2 mL) and added slowly to the stirring solution of (dppp)$PtPh_2$. After addition was complete, the reaction was stirred for 10 min. Volatiles were removed under reduced pressure, and the mixture was triturated and washed with petroleum ether [2 × 2 mL]. The resulting white solids were dried under reduced pressure, providing off-white **18** (54.0 mg, 89.3%).

$^1H$ NMR (300 MHz, $CD_2Cl_2$): $\delta$ 7.7 (4H, m), 7.6 (6H, m), 7.4 (6H, m), 7.3 (4H, m), 7.0 (2H, m), 6.7 (3H, m), 3.33 (4H, m), 2.75 (4H, m), 1.7 (2H, m), 1.18 (4H, m). $^{13}C\{^1H\}$ NMR (125.7 MHz, $CD_2Cl_2$): $\delta$ 158.9 (dd), 149.7, 147.8, 139.8, 137.9, 136.0, 133.6 (d), 133.4 (d), 132.4, 130.0 (d), 129.3 (d), 128.5 (d), 125.1, 73.0, 27.2 (d), 27.1 (d), 24.6, 18.6. $^{31}P\{^1H\}$ NMR (121.4 MHz, $CD_2Cl_2$): $\delta$ 12.0 (d, $J_{P-P}$ = 22.5 Hz, $J_{Pt-P}$ = 1620 Hz), −3.0 (d, $J_{P-P}$ = 22.5 Hz, $J_{Pt-P}$ = 4524 Hz). $^{19}F\{^1H\}$ NMR (282 MHz, $CD_2Cl_2$): $\delta$ −133.5, −163.9, −167.7. $^{11}B\{^1H\}$ NMR (128 MHz, $CD_2Cl_2$): $\delta$ −19.1. Anal. Calcd. for $C_{61}H_{39}BF_{20}$-$OP_2Pt$: C, 51.03; H, 2.74. Found: C, 51.21; H, 2.74.

**[{($Ph_2SiP_2$)Pt}$_2$($\mu$-$\eta^3$:$\eta^3$-biphenyl)][B($C_6F_5$)$_4$]$_2$ (19).** Thermolysis of **14** (24.5 mg, 15.9 $\mu$mol) in benzene at 55 °C for 24 h resulted in the formation a single product as evidenced by $^{31}P$ NMR. Isolation of orange solids by removal of volatiles under reduced pressure followed by washing with petroleum ether [2 × 2 mL] provided **19** (21.7 mg, 89.1%). Crystals of **19** were obtained by slow cooling of a saturated solution of **19** in *o*-xylene.

$^1H$ NMR (300 MHz, acetone-$d_6$): $\delta$ 7.77 (1H, m), 7.49 (16H, m), 7.27 (28H, m), 7.15 (2H, m), 7.10 (8H, m), 6.92 (8H, m), 6.54 (2H, d), 5.64 (m, 1H), 4.24 (2H, bd), 4.03 (2H, bt), 2.73 (8H, d, $J_{P-H}$ = 13.2 Hz, $J_{Pt-H}$ = 62.4 Hz). $^{13}C\{^1H\}$ NMR (125.7 MHz, acetone-$d_6$): $\delta$ 150.6, 148.7, 140.6, 138.7, 135.1, 134.1, 133.6, 132.9, 130.5, 129.3, 126.5, 107.4, 95.7, 81.2, 76.1, 9.3. $^{31}P\{^1H\}$ NMR (121.4 MHz, acetone-$d_6$): $\delta$ 8.42 ($J_{Pt-P}$ = 3940 Hz). $^{19}F\{^1H\}$ NMR (282 MHz, acetone-$d_6$): $\delta$ −132.5, −163.6 (t), −167.6. ES MS: $m/z$ 852.8 ([$M^{2+}$]). Anal. Calcd. for $C_{136}H_{78}B_2$-$F_{40}P_4Pt_2Si_2$: C, 53.31; H, 2.57. Found: C, 51.82; H, 2.35.

**[{(dppp)Pt}$_2$($\mu$-$\eta^3$:$\eta^3$-biphenyl)][B($C_6F_5$)$_4$]$_2$ (20).** Thermolysis of **18** (32.7 mg, 22.8 $\mu$mol) in benzene at 55 °C for 4 h

resulted in the formation of two products as evidenced by $^{31}$P NMR. Removal of volatiles under reduced pressure provided a mixture of **20** and a second species which is presumed to be the hydroxy-bridged dimer, $[(dppp)Pt(\mu\text{-}OH)]_2[B(C_6F_5)_4]_2$. Spectral analysis was consistent with the formulation of the major product as **20** by comparison to **19** and previously reported systems.[12]

$^1$H NMR (300 MHz, $CD_2Cl_2$): $\delta$ 6.6−7.8 (aryl protons), 5.15 (m, 1H), 4.21 (br, 2H), 3.67 (br, 2H), 2.63 (br, 8H), 1.64 (m, 4H). $^{31}$P{$^1$H} NMR (121.4 MHz, $CD_2Cl_2$): $\delta$ 0.20 ($J_{Pt-P}$ = 3737 Hz). $^{19}$F{$^1$H} NMR (282 MHz, $CD_2Cl_2$): $\delta$ −133.4, −163.7 (t), −167.5.

**[[$Ph_2BP_2$]Pt($Ph$)$_2$][ASN] (21).** A THF solution (2 mL) of (COD)Pt($C_6H_5$)$_2$ (45.5 mg, 99.5 $\mu$mol) was added to a stirring suspension of [$Ph_2BP_2$][ASN] (68.6 mg, 99.5 $\mu$mol) in THF (3 mL). The reaction was stirred for 1 h, during which the mixture became a homogeneous solution. The solution was concentrated and triturated with pentane [3 × 2 mL]. The resulting off-white solids were dried under reduced pressure, providing **21** (101.0 mg, 97.7%).

$^1$H NMR (300 MHz, $CD_3CN$): $\delta$ 7.21 (m, 8H), 7.01 (m, 4H), 6.90 (m, 12H), 6.80 (m, 4H), 6.60 (m, 4H), 6.53 (m, 2H), 6.30 (m, 4H), 6.18 (m, 2H), 3.28 (m, 8H), 2.08 (m, 8H), 2.02 (br, 4H). $^{13}$C{$^1$H} NMR (125.7 MHz, $CD_3CN$): $\delta$ 168.3 (dd, *ipso* Pt($C_6H_5$)$_2$, $^2J_{P-C(trans)}$ = 111 Hz, $^2J_{P-C(cis)}$ = 12 Hz), 165, 138.5, 137.4 (s, *ortho* Pt($C_6H_5$)$_2$, $^2J_{Pt-C}$ = 29 Hz), 133.8, 132.4, 127.9, 126.9 (s, *meta* Pt($C_6H_5$)$_2$, $^3J_{Pt-C}$ = 8.9 Hz), 126.2, 126.0, 121.6, 119.4, 63.3, 22.3, 20.3 (br). $^{31}$P{$^1$H} NMR (121.4 MHz, $CD_3CN$): $\delta$ 13.99 ($^1J_{Pt-P}$ = 1772 Hz). $^{11}$B{$^1$H} NMR (128.3 MHz, $CD_3CN$): $\delta$ −14.4. ES MS: *m/z* 912.3 ([M$^-$]). Anal. Calcd. for $C_{58}H_{60}BNP_2Pt$: C, 67.05; H, 5.82; N, 1.35. Found: C, 66.23; H, 5.96; N, 1.48.

**($Ph_2SiP_2$)Pt($Ph$)$_2$ (22).** Solid $Ph_2SiP_2$ (70.3 mg, 0.121 mmol) and $CODPtPh_2$ (55.4 mg, 0.121 mmol) were dissolved in THF (2 mL). After 20 min, volatiles were removed under reduced pressure. The resulting solids were triturated with petroleum ether (3 mL), and the solution was decanted. The resulting off-white solids were dried under reduced pressure, providing **22** (103.2 mg, 91.7%).

$^1$H NMR (300 MHz, $CDCl_3$): $\delta$ 7.36 (m, 8H), 7.18 (m, 6H), 7.05 (m, 12H), 6.93 (m, 4H), 6.87 (m, 4H), 6.44 (m, 4H), 6.31 (m, 2H), 2.41 (d, 4H, $J_{P-H}$ = 9.6 Hz, $J_{Pt-H}$ = 33 Hz). $^{13}$C{$^1$H} NMR (125.7 MHz, $CDCl_3$): $\delta$ 162.7 (dd, $J_{P-C}$ = 12, 113 Hz), 136.1 ($J_{Pt-C}$ = 31 Hz), 135.2, 133.7, 133.3 (m), 129.7, 127.9, 127.8 (m), 126.8 ($J_{Pt-C}$ = 66 Hz), 120.3, 9.7 (m). $^{31}$P{$^1$H} NMR (121.4 MHz, $CDCl_3$): $\delta$ 6.02 ($J_{Pt-P}$ = 1720 Hz). Anal. Calcd. for $C_{50}H_{44}P_2PtSi$: C, 64.57; H, 4.77. Found: C, 64.73; H, 5.12.

**[$Ph_2BP_2$]Pt(Me){P($C_6F_5$)$_3$} (25).** A THF solution (2 mL) of **13** (104.5 mg, 123.6 $\mu$mol) was added to solid P($C_6F_5$)$_3$ (66.1 mg, 124.2 $\mu$mol). The resulting solution was concentrated under reduced pressure. Toluene (4 mL) was added, and the solution was concentrated under reduced pressure. Petroleum ether (2 mL) was added, forming a white precipitate, which was collected by filtration and washed with additional petroleum ether (2 mL). The solids were dissolved in benzene (2 mL), and the solution was filtered. Volatiles were removed under reduced pressure, providing white solid **25** (133.2 mg, 82.5%). Crystals suitable for X-ray diffraction were grown from petroleum ether diffusion into a benzene solution of **25**.

$^1$H NMR (300 MHz, $C_6D_6$): $\delta$ 7.44 (br, 4H), 7.26−7.30 (br, 8H), 7.06 (m, 6H), 6.93 (br, 6H), 6.81 (br, 6H), 2.63 (br d, 2H, $J_{P-H}$ = 15 Hz, $J_{Pt-H}$ = 53 Hz), 2.24 (dd, 2H, $J_{P-H}$ = 10, 14 Hz, $J_{Pt-H}$ = 59 Hz), 0.04 (ddd, 3H, $J_{P-H}$ = 5.4, 5.4, 11 Hz, $J_{Pt-H}$ = 54 Hz). $^{13}$C{$^1$H} NMR (125.7 MHz, $C_6D_6$): $\delta$ 163 (br), 148.3, 146.2, 145.1, 143.0, 138.9, 136.9, 133.9, 132.8, 130.2, 129.9, 128, 127.1, 123.1, 103.6, 23.4, 19.8, 0.75 (br d, $^1J_{Pt-C}$ = 500 Hz, $^2J_{P-C(trans)}$ = 69 Hz). $^{31}$P{$^1$H} NMR (121.4 MHz, $C_6D_6$): $\delta$ 22.83 (dd, $^1J_{Pt-P}$ = 3139 Hz, $^2J_{P-P}$ = 29.9, 433 Hz), 18.84 (dd, $^1J_{Pt-P}$ = 1945 Hz, $^2J_{P-P}$ = 17.1, 29.2 Hz), −17.97 (br d, $^1J_{Pt-P}$ = 2499 Hz, $^2J_{P-P}$ = 430 Hz). $^{11}$B{$^1$H} NMR (128.3 MHz, $C_6D_6$): $\delta$ −19.1. $^{19}$F{$^1$H} NMR (282.1 MHz, $C_6D_6$): $\delta$ −124.5 (br sh), −127.0 (br), −135.2 (br), −145.4 (br), −155.4 (br sh), −157.6 (br), −159.6 (br). Anal. Calcd. for $C_{57}H_{37}BF_{15}P_3Pt$: C, 52.43; H, 2.86. Found: C, 52.51; H, 2.63.

**[$Ph_2BP_2$]Pt(Ph){P($C_6F_5$)$_3$} (26).** Thermolysis of **25** (43.2 mg) in benzene (0.7 mL) at 80 °C over 24 h led to the quantitative formation of **26**.

$^1$H NMR (300 MHz, $C_6D_6$): $\delta$ 6.2−7.8 (35H, aryl protons), 2.0−2.8 (br, 4H). $^{31}$P{$^1$H} NMR (121.4 MHz, $C_6D_6$): $\delta$ 17.92 (dd, $J_{P-P}$ = 28, 419 Hz, $J_{Pt-P}$ = 3132 Hz), 10.85 (br m, $J_{Pt-P}$ = 1770 Hz), −24.01 (br d, $J_{P-P}$ = 422 Hz, $J_{Pt-P}$ = 2462 Hz). $^{11}$B{$^1$H} NMR (128.3 MHz, $C_6D_6$): $\delta$ −15.5. $^{19}$F{$^1$H} NMR (282.1 MHz, $C_6D_6$): $\delta$ −126.4 (br), −129.5 (br), −133.1 (br), −145 (br), −158.3 (br), −160.1 (br). Anal. Calcd. for $C_{62}H_{39}BF_{15}P_3Pt$: C, 54.44; H, 2.87. Found: C, 54.58; H, 2.62.

**[[$Ph_2BP_2$]Pt(Me)(Ph)][ASN] (27).** A THF solution (1 mL) of (COD)Pt(Me)(Ph) (70.6 mg, 0.179 mmol) was added to a stirring suspension of [$Ph_2BP_2$][ASN] (123.1 mg, 0.1785 mmol) in THF (2 mL). The reaction was stirred for 30 min and became homogeneous. The solution was concentrated under reduced pressure, and off-white solids were precipitated with diethyl ether (2 mL). The supernatant was removed, and the solids were washed with ethanol [2 × 2 mL] and diethyl ether [2 × 2 mL] and dried under reduced pressure, producing off-white **27** (122.4 mg, 70.2%).

$^1$H NMR (300 MHz, acetone-$d_6$): $\delta$ 7.47 (m, 4H), 7.24 (m, 4H), 7.12 (m, 2H), 7.09 (m, 4H), 6.98 (m, 4H), 6.87 (m, 8H), 6.62 (m, 4H), 6.57 (m, 2H), 6.43 (m, 2H), 6.29 (m, 1H), 3.69 (m, 8H,), 2.26 (m, 8H), 2.10 (br, 2H), 2.02 (br, 2H), 0.08 (dd, 3H, $^3J_{P-H(cis)}$ = 6.9 Hz, $^3J_{P-H(trans)}$ = 7.8 Hz, $^2J_{Pt-H}$ = 69 Hz). $^{13}$C{$^1$H} NMR (125.7 MHz, acetone-$d_6$): $\delta$ 166 (br), 144, 140.5 (d), 139.8 (d), 138.7, 135.0 (m), 134.7 (m), 133.8, 128.9, 128.4, 127.9 (d), 127.5 (d), 127.0, 126.8, 122.4, 120.0, 64.3, 23.3, 23 (br), 22 (br), 5.5 (dd, $^2J_{P-C(trans)}$ = 93 Hz). $^{31}$P{$^1$H} NMR (121.4 MHz, acetone-$d_6$): $\delta$ 18.3 (d, $^1J_{Pt-P}$ = 1775 Hz, $^2J_{P-P}$ = 19 Hz), 17.29 (d, $^1J_{Pt-P}$ = 1868 Hz, $^2J_{P-P}$ = 19 Hz). $^{11}$B{$^1$H} NMR (128.3 MHz, acetone-$d_6$): $\delta$ −13.8. Anal. Calcd. for $C_{53}H_{57}BNP_2Pt$: C, 65.16; H, 5.98; N, 1.43. Found: C, 64.90; H, 6.05; N, 1.54.

**($Ph_2SiP_2$)Pt(Me)(Ph) (28).** Solid **2** (39.7 mg, 68.4 $\mu$mol) and CODPt(Me)(Ph) (27.0 mg, 68.3 $\mu$mol) were dissolved in THF (2 mL) and stirred for 10 min. Volatiles were removed under reduced pressure, and the mixture was triturated with petroleum ether [3 × 3 mL]. The resulting off-white solids were dried under reduced pressure to provide **28** (52.6 mg, 88.7%).

$^1$H NMR (300 MHz, $C_6D_6$): $\delta$ 7.64 (m, 4H), 7.53 (m, 2H), 7.39 (m, 4H), 7.04−6.80 (m, 25H), 2.27 (d, 2H, $^2J_{P-H}$ = 10.8 Hz), 2.19 (d, 2H, $^2J_{P-H}$ = 11.4 Hz), 1.09 (dd, 3H, Pt(C$H_3$), $^3J_{P-H}$ = 7.2 Hz, $^3J_{P-H}$ = 9.6 Hz, $^2J_{Pt-H}$ = 70 Hz). $^{31}$P{$^1$H}

NMR (121.4 MHz, $C_6D_6$): $\delta$ 8.96 ($^1J_{Pt-P}$ = 1792 Hz, $^2J_{P-P}$ = 14 Hz), 8.08 ($^1J_{Pt-P}$ = 1715 Hz, $^2J_{P-P}$ = 14 Hz). Anal. Calcd. for $C_{45}H_{42}P_2PtSi$: C, 62.27; H, 4.88. Found: C, 61.47; H, 4.87.

**[(Ph$_2$SiP$_2$)Pt(Me){P(C$_6$F$_5$)$_3$}][B(C$_6$F$_5$)$_4$] (29).** Solid **14** (29.0 mg, 18.8 $\mu$mol) was dissolved in dichloromethane (2 mL) with $P(C_6F_5)_3$(10.0 mg, 18.8 $\mu$mol) and the solution was stirred for 10 min. Volatiles were removed under reduced pressure. The resulting solids were triturated with toluene (2 mL), washed with petroleum ether [2 × 2 mL], and dried under reduced pressure, providing **29** (29.7 mg, 79.0%).

$^1$H NMR (300 MHz, $CD_2Cl_2$): $\delta$ 7.40 (br), 7.32 (m), 7.28 (m), 7.13 (t, 4H), 6.93 (d, 4H), 2.58 (d, 2H, $^2J_{P-H}$ = 12.9 Hz, $^3J_{Pt-H}$ = 34 Hz), 2.15 (dd, 2H, $^2J_{P-H}$ = 5.7 Hz, $^2J_{P-H}$ = 15.0 Hz, $^3J_{Pt-H}$ = 48 Hz), 0.03 (ddd, 3H, $^3J_{P-H}$ = 6.6, 10.8, 12.0 Hz, $^2J_{Pt-H}$ = 51 Hz). $^{13}$C{$^1$H} NMR (125.7 MHz, $CD_2Cl_2$): $\delta$ 149.7, 148.4, 147.8, 146.4, 143.9, 139.5, 137.9, 135.9, 134.0, 133.8, 132.9, 132.4, 130.9, 129.4, 128.9, 124.3, 102.2, 11.8, 9.8, 5.8 (m). $^{31}$P{$^1$H} NMR (121.4 MHz, $CD_2Cl_2$): $\delta$ 13.09 (dd, $^2J_{P-P}$ = 449, 27.5 Hz, $^1J_{Pt-P}$ = 3246 Hz), 9.37 (dd, $^2J_{P-P}$ = 21.4, 27.5 Hz, $^1J_{Pt-P}$ = 1984 Hz), −19.03 (br d, $^2J_{P-P}$ = 443 Hz, $^1J_{Pt-P}$ = 2796 Hz). $^{19}$F{$^1$H} NMR (282 MHz, $CD_2Cl_2$): $\delta$ −126.9 (br), −133.7, −143.7 (br), −157.7 (br), −163.9, −167.8. Anal. Calcd. for $C_{81}H_{37}BF_{35}P_3PtSi$: C, 48.59; H, 1.86. Found: C, 46.88; H, 2.09.

**[(Ph$_2$SiP$_2$)Pt(Ph){P(C$_6$F$_5$)$_3$}][B(C$_6$F$_5$)$_4$] (30).** Solid **21** (26.5 mg, 28.5 $\mu$mol) was dissolved in dichloromethane (1 mL) with $P(C_6F_5)_3$ (15.2 mg, 28.6 $\mu$mol). While stirring, a dichloromethane solution (1 mL) of $[H(Et_2O)_2][B(C_6F_5)_4]$ (23.3 mg, 28.5 $\mu$mol) was added slowly. After 10 min, volatiles were removed under reduced pressure. The solids were washed with petroleum ether [2 × 2 mL] and dried under reduced pressure (51.4 mg). The resulting solids were composed of 90−95% **30** and 5−10% **19**; therefore, elemental analysis was not obtained.

$^1$H NMR (300 MHz, $CD_2Cl_2$): $\delta$ 7.0−7.6, 6.77 (m), 6.46 (m), 6.23 (br), 2.64 (br, 2H), 2.33 (br, 2H). $^{31}$P{$^1$H} NMR (121.4 MHz, $CD_2Cl_2$): $\delta$ 6.79 (dd, $J_{P-P}$ = 25, 445 Hz, $J_{Pt-P}$ = 3319 Hz), 3.04 (dd, $J_{P-P}$ = 19, 25 Hz, $J_{Pt-P}$ = 1870 Hz), 26.61 (dd, $J_{P-P}$ = 19, 440 Hz, $J_{Pt-P}$ = 2785 Hz). $^{19}$F{$^1$H} NMR (282 MHz, $CD_2Cl_2$): $\delta$ −124.3 (br), −133.5, −144.1 (br), −158.2 (br), −163.9, −167.8.

**MeP(C$_6$D$_5$)$_2$ (31).** $C_6D_5Br$ (10.0533 g, 62.034 mmol) was reacted with $Mg^0$ (3.033 g, 124.8 mmol) in $Et_2O$ at reflux over 2h to form the aryl Grignard reagent. The solution was transferred by cannula to a Schlenk flask containing $MePCl_2$ (3.6193 g, 30.953 mmol) in $Et_2O$ (100 mL) at −78 °C. The reaction was stirred and warmed gradually over 4h. Volatiles were removed under reduced pressure, and the resulting sludge was extracted with petroleum ether (100 mL) and filtered. The solution was concentrated under reduced pressure, providing **31** (2.702 g, 41%).

$^1$H NMR (300 MHz, $CDCl_3$): $\delta$ 1.65 (d, $J_{P-H}$ = 3.3 Hz). $^{31}$P{$^1$H} NMR (121.4 MHz, $CDCl_3$): $\delta$ −26.9. GC MS: *m/z* 210 ([M$^+$]).

**THF Exchange Experiments.** A known amount (ca. 20 mg) of methyl solvento complex **13** or **14** was dissolved in $C_6D_6$ with a known concentration (3−15 equiv) of THF in a J. Young tube. The temperature of the probe on a Varian Inova 500 spectrometer was equilibrated and determined using the temperature-dependent peak separation of methanol or ethylene glyocol. The J. Young tube was inserted into the probe and allowed to thermally equilibrate. The 90° pulse width of the peak to be inverted (downfield peak of free THF, ∼3.6 ppm) was determined before each experiment at the appropriate temperature. Magnetization transfer experiments were performed using the DANTE pulse sequence[23] and selectively inverting the downfield free THF peak. The peak areas for free and bound THF were measured after different pulse-mixing times (30 $\mu$s to 50 s) using a nonselective 90° pulse. Between 25 and 40 data points were acquired as four repetitions with a 50 s relaxation delay. The rate of exchange was determined using the CIFIT computer program.[24]

**Kinetics Experiments.** In a typical experiment, 20−30 mg of the appropriate methyl solvento complex (**13**−**15**) or methyl phosphine complex (**25**) (and when appropriate, [$^n$Bu$_4$N][B(C$_6$F$_5$)$_4$] or THF) was dissolved in $C_6H_6$ or $C_6D_6$ (0.64 mL) and filtered into a J. Young tube holding a capillary containing an internal integration standard ($PMe_3$ ($^{31}$P NMR) or $Cp_2Fe$ ($^1$H NMR) in $C_6D_6$). The sealed tube was then heated in a temperature equilibrated heating block or in the NMR probe. Heating block temperature was calibrated using a thermocouple device, and NMR probe temperature was calibrated using an ethylene glycol standard. The reaction was monitored either by $^{31}$P NMR and integrating the most downfield peak (corresponding to the ligated phosphorus atom trans to the methyl ligand in each case) versus the internal standard ($PMe_3$), or by $^1$H NMR and integrating the peak corresponding to the methyl ligand versus the internal standard ($Cp_2Fe$). The resulting data was fit to a pseudo-first-order decay of the methyl solvento species. Each experiment was repeated in triplicate. The value of the rate constant is an average of three experimental results, and the error reported is the standard deviation of the three observed rate constants.

**Acknowledgment.** The authors acknowledge financial support from the NSF (CHE-0132216), BP, and the ACS PRF. J.C.T. is grateful for an NSF graduate fellowship and a Moore fellowship. Dr. Michael Day, Lawrence Henling, and Theodore Betley are acknowledged for assistance with crystallographic studies. Prof. John Bercaw, Dr. Alan Heyduk, Dr. Gregory Kubas, and Dr. Jennifer Love are acknowledged for insightful discussions.

**Note Added after ASAP:** The version published on the Web 06/17/2003 was not the corrected version. The version published on the Web 06/25/2003 and the print version are correct.

**Supporting Information Available:** Crystallographic experimental details for complexes **7**, **8**, **9**, **13**, **19**, and **25**,[44] additional graphs of kinetic results, and $^{31}$P{$^1$H} NMR figures of **14** and **15**. This material is available free of charge via the Internet at http://pubs.acs.org.

JA0296071

(44) Crystallographic data have been deposited at the CCDC, 12 Union Road, Cambridge CB2 1EZ, UK, and copies can be obtained on request, free of charge, by quoting the publication citation and the deposition number 151640 (**7**), 198492 (**8·toluene**), 198491 (**9**), 156632 (**13·2THF**), 186231 (**19·4(*o*-xylene)**), 198490 (**25·benzene**).